MICROBIOLOGY

Switching from membrane disrupting to membrane crossing, an effective strategy in designing antibacterial polypeptide

Haodong Zhang[1]†, Qi Chen[2]†, Jiayang Xie[2]†, Zihao Cong[2], Chuntao Cao[2], Wenjing Zhang[2], Donghui Zhang[1], Sheng Chen[2], Jiawei Gu[2], Shuai Deng[2], Zhongqian Qiao[2], Xinyue Zhang[2], Maoquan Li[3], Ziyi Lu[2], Runhui Liu[1,2]*

Drug-resistant bacterial infections have caused serious threats to human health and call for effective antibacterial agents that have low propensity to induce antimicrobial resistance. Host defense peptide–mimicking peptides are actively explored, among which poly-β-L-lysine displays potent antibacterial activity but high cytotoxicity due to the helical structure and strong membrane disruption effect. Here, we report an effective strategy to optimize antimicrobial peptides by switching membrane disrupting to membrane penetrating and intracellular targeting by breaking the helical structure using racemic residues. Introducing β-homo-glycine into poly-β-lysine effectively reduces the toxicity of resulting poly-β-peptides and affords the optimal poly-β-peptide, βLys$_{50}$HG$_{50}$, which shows potent antibacterial activity against clinically isolated methicillin-resistant *Staphylococcus aureus* (MRSA) and MRSA persister cells, excellent biosafety, no antimicrobial resistance, and strong therapeutic potential in both local and systemic MRSA infections. The optimal poly-β-peptide demonstrates strong therapeutic potential and implies the success of our approach as a generalizable strategy in designing promising antibacterial polypeptides.

INTRODUCTION

Drug-resistant bacteria have emerged quickly in recent years because of the intensive use of antibiotics, which has been a serious problem globally (*1*, *2*). Methicillin-resistant *Staphylococcus aureus* (MRSA) are a class of important pathogen for nosocomial and community-acquired infections (*3*, *4*). Because of antibiotic resistance, MRSA can frequently cause serious and even life-threatening infections such as blood infection, pneumonia, skin and organ infections, and bone infection (*5*–*7*). Therefore, it is urgent to develop antimicrobial agents that have potent activity against MRSA and low probability to induce bacteria to develop resistance (*8*, *9*).

Host defense peptides (HDPs) are considered as promising candidates in developing antimicrobials owing to HDPs' broad-spectrum antibacterial activity and insusceptibility to antimicrobial resistance (*10*–*12*). However, the application of HDPs is limited because of their inherent shortcomings such as low stability upon proteolysis, tedious and time-consuming synthesis, and high production cost (*13*, *14*). To overcome the disadvantages of HDPs, synthetic mimics of HDPs have been explored as antibacterial agents to show promising activities (*15*–*30*). Poly-β-peptides are considered to be one of the most promising antimicrobial agents among

these mimics, and the Gellman laboratory contributes substantially to this field by exploring the relationships between peptide structures and antimicrobial functions (*31*–*33*). Among these poly-β-peptides, poly-β-L-lysine (*34*) is known to have potent antibacterial activity but poor selectivity due to its high cytotoxicity (*35*, *36*) to mammalian cells. Poly-β-L-lysine adopts the α-helical structure and has a strong interaction with cell membrane to have a membrane disruption mechanism (Fig. 1A) (*34*), which is similar to the observation in poly-α-peptides that the α-helical structure easily breaks membrane integrity (*37*, *38*). The poor selectivity of membrane-disrupting helical poly-β-L-lysine inspires us to design selective antibacterial polypeptides with a different mode of action (*39*), switching from membrane disrupting to membrane crossing and targeting the intracellular objects.

Recently, we found that poly(2-oxazoline)s can work as functional mimics of HDPs (*40*–*42*), among which some heterochiral peptide-mimicking polymers have weak interaction with cell membrane and cross the bacterial membrane to target intracellular objects (*40*). These heterochiral poly(2-oxazoline)s adopt random coil conformation and exert selective antibacterial activity, which inspires us to explore heterochiral poly-β-DL-lysine (poly-β-lysine; Fig. 1A) that loses the helical structure of poly-β-L-lysine and is assumed to have reduced interaction with cell membrane. With this design, we find that poly-β-lysine has weak interaction with membrane and kills bacteria by penetrating the membrane to target intracellular objects. By introducing β-homo-glycine residue into poly-β-lysine, we obtain poly-β-peptides with reduced charge density and reduced cytotoxicity compared to poly-β-lysine (Fig. 1A) (*43*). The optimal poly-β-peptide, βLys$_{50}$HG$_{50}$, shows low hemolysis and cytotoxicity, insusceptibility to antibacterial resistance, as well as potent antibacterial activity against MRSA and strong therapeutic potential for MRSA-

[1]State Key Laboratory of Bioreactor Engineering, East China University of Science and Technology, Shanghai 200237, China. [2]Key Laboratory for Ultrafine Materials of Ministry of Education, Frontiers Science Center for Materiobiology and Dynamic Chemistry, Research Center for Biomedical Materials of Ministry of Education, Shanghai Frontiers Science Center of Optogenetic Techniques for Cell Metabolism, School of Materials Science and Engineering, East China University of Science and Technology, Shanghai 200237, China. [3]Department of Interventional and Vascular Surgery, Shanghai Tenth People's Hospital, Tongji University School of Medicine, Shanghai 200072, China.
†These authors contributed equally to this work.
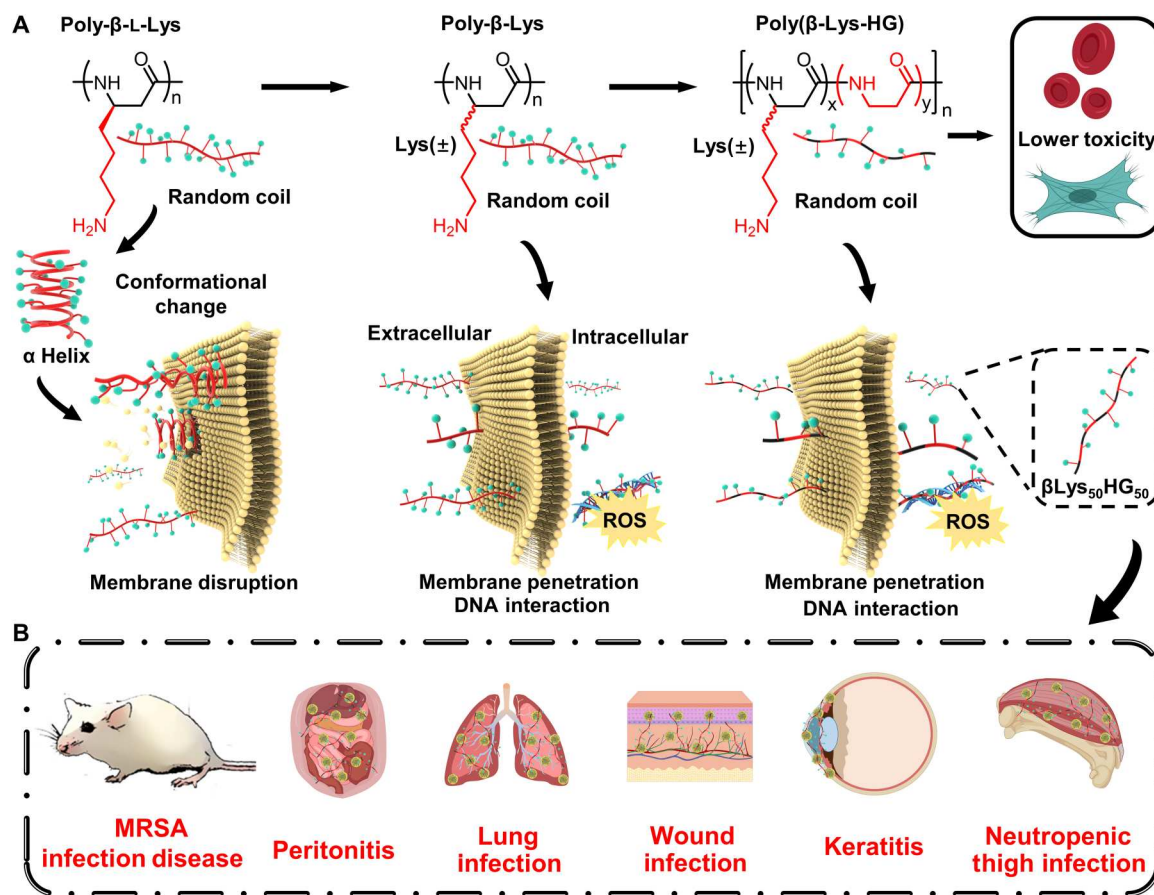*Corresponding author. Email: rliu@ecust.edu.cn

Fig. 1. The strategy of designing low-toxicity poly-β-peptides, by switching the antibacterial mechanism, to address the challenge of infectious diseases. (**A**) Design of poly-β-peptides with effective antibacterial activity and low toxicity by changing the interaction mechanism between peptide and bacterial membrane. (**B**) The poly-β-peptides optimized by the above strategy have shown excellent therapeutic potential in a variety of in vivo MRSA infection models, including full-thickness wound infection, keratitis, neutropenic thigh infection, lung infection, and systemic peritonitis infection.

induced infections in five murine infection models (Fig. 1B). Moreover, this optimal poly-β-peptide kills bacteria by penetrating the membrane to generate intracellular reactive oxygen species (ROS) and interact with DNA, rather than disrupting the membrane directly, which validates the proposed strategy in designing potent and selective antibacterial poly-β-peptides by switching the mode of action from membrane disrupting to membrane penetrating.

RESULTS
Synthesis of β-lactam monomers
To prepare poly-β-peptides, we synthesized two monomers, the β-homo-lysine lactam (Lys-β-lactam) and β-homo-glycine lactam (HG-β-lactam). Lys-β-lactam was synthesized through a three-step reaction from 6-bromo-1-hexene to give the final product (Fig. 2A and figs. S1 to S4). Compared to the synthesis of Lys-β-lactam in precedent literatures (*44*), generally involving a six-step reaction and using Mukaiyama reagent for ring closure to obtain L-Lys-β-lactam (figs. S9 to S13), our synthesis here is concise and easy to scale up, which avoids using hazardous reagents such as diazomethane and Pd/C. HG-β-lactam was synthesized from vinyl acetate via a ring-closure step followed by reduction to give the final product (Fig. 2B and figs. S5 to S8).

Design, synthesis, and characterization of poly-β-peptides
The random poly-β-peptides were synthesized via an anionic ring-opening polymerization on a mixture of Lys-β-lactam and HG-β-lactam in variable ratios, with Lys-β-lactam increasing incrementally from 50 to 100%, with an expected chain length of 20 amino acid residues (Fig. 2C). The random property of the resulting polypeptide was confirmed by the similarly quick consumption rate of both monomers in the copolymerization reaction (figs. S24 and S25). After removing the protecting groups using trifluoroacetic acid (TFA) with triethylsilane (Et₃SiH), final poly-β-peptides βLys_xHG_y ($x + y = 100\%$, $x = 50, 60, 70, 80, 90, 100\%$) were obtained as TFA salts. Proton nuclear magnetic resonance (^1H NMR) characterization confirmed the actual ratio change of residues within the poly-β-peptide chain (Fig. 2D and figs. S14 to S19). Gel permeation chromatography (GPC) characterization showed that these poly-β-peptides have polymer lengths of ~20 residues [Degree of Polymerization (DP) = 16 to 23] and dispersities (Đ) of 1.11 to 1.46 (Fig. 2E and fig. S26). The polymer lengths obtained from GPC characterization were close to those obtained from terminal analysis using ^1H NMR. To have close comparison between the heterochiral poly-β-lysine and helical poly-β-lysine (poly-β-L-lysine), we also synthesized poly-β-L-lysine (fig. S20).

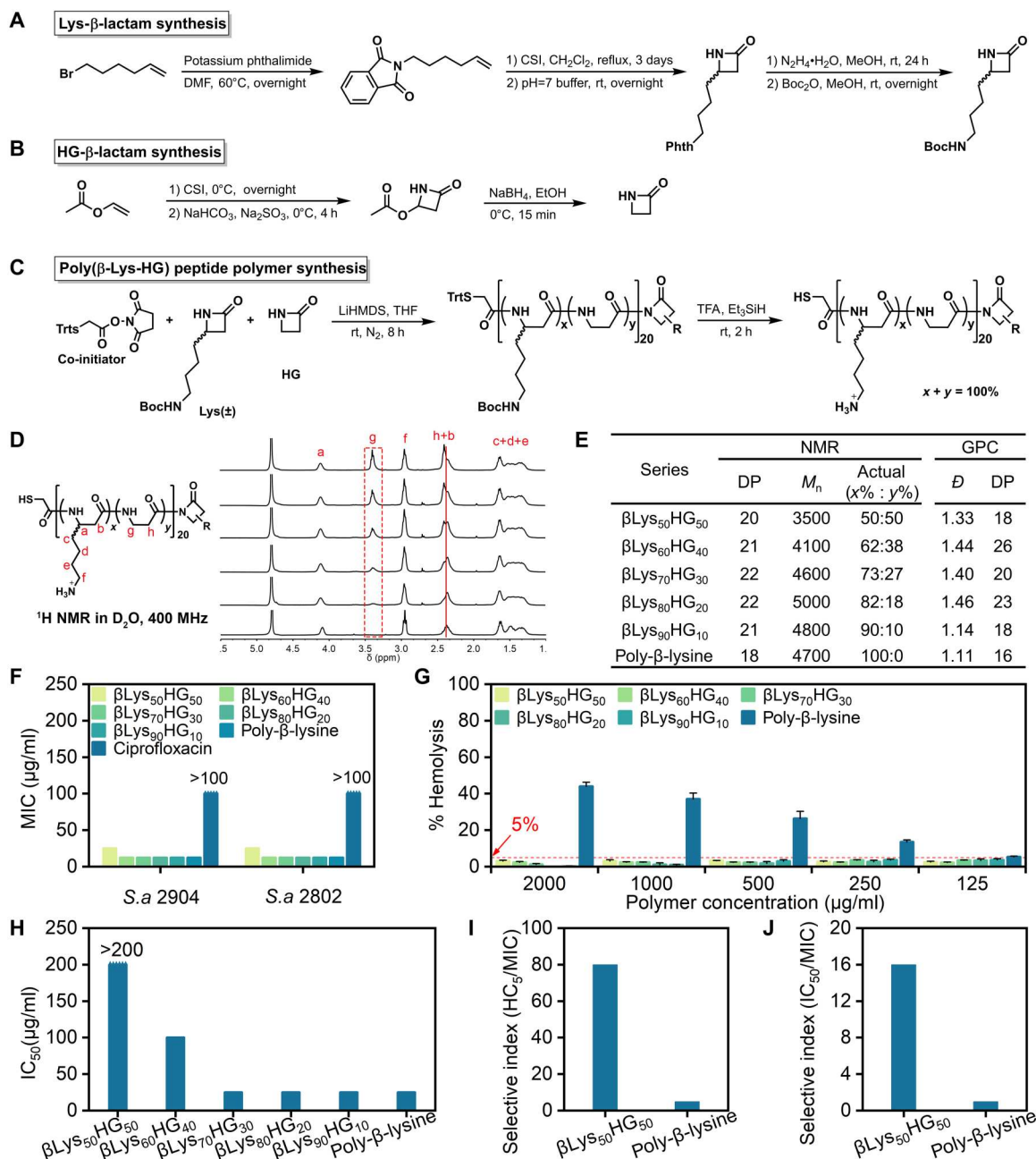**Fig. 2. Poly-β-peptide synthesis, antimicrobial activity, and biocompatibility in vitro.** (**A** and **B**) Synthetic route of Lys-β-lactam and HG-β-lactam. (**C**) Synthesis of poly-β-peptides, which are under protection. R represents the side chain of the Lys or HG subunit. (**D** and **E**) Proton nuclear magnetic resonance (^{1}H NMR) spectrum and gel permeation chromatography (GPC) measurements of poly-β-peptide ($x + y = 100\%$, $x = 50, 60, 70, 80, 90,$ and 100%). (**F**) Antimicrobial activity of poly-β-peptides, using ciprofloxacin for comparison. (**G**) Hemolytic activity of poly-β-peptides; the red dashed line represents the minimum concentration causing 5% hRBC loss (HC$_5$) value. (**H**) Cell cytotoxicity of poly-β-peptides. (**I**) Selectivity index of βLys$_{50}$HG$_{50}$ and poly-β-lysine calculated from IC$_{50}$/MIC. (**J**) Selectivity index of βLys$_{50}$HG$_{50}$ and poly-β-lysine calculated from HC$_5$/MIC. Data are presented as means ± SD. rt, room temperature; ppm, parts per million.

Identification of the optimal poly-β-peptide βLys$_{50}$HG$_{50}$

We examined these poly-β-peptides for their antibacterial activity against MRSA using two clinically isolated strains of MRSA, *S. aureus* 2904 and *S. aureus* 2802, both of which are resistant to all 19 antibiotics in our test, such as methicillin, ceftriaxone, vancomycin, and ciprofloxacin (fig. S27). All these poly-β-peptides displayed potent activities against these two strains of MRSA, with a minimum inhibitory concentration (MIC) of 12.5 μg/ml in most cases (Fig. 2F). Hemolysis study using human red blood cells (hRBCs) showed that poly-β-lysine displays substantial hemolysis at a concentration of more than 250 μg/ml; in contrast, incorporation of HG residue effectively reduced hemolysis of all poly(β-Lys-HG) to less than 5% (HC$_5$) even at a peptide concentration of 2000 μg/ml (Fig. 2G). Cytotoxicity study showed that incorporation of

more than 40% HG residue substantially reduced cytotoxicity of poly-β-peptides to NIH-3T3 fibroblasts, displaying the minimum concentration to cause 50% loss in cell viability [median inhibitory concentration (IC_{50})] greater than 200 μg/ml for $\beta Lys_{50}HG_{50}$ (Fig. 2H). In addition, antibacterial selectivity indices were calculated regarding hemolysis (HC_5/MIC) and cytotoxicity (IC_{50}/MIC), respectively. These analyses showed that the incorporation of HG residue into poly-β-lysine at an appropriate ratio can retain the antibacterial activity and substantially reduce hemolysis and cytotoxicity. The optimal poly-β-peptide was identified as $\beta Lys_{50}HG_{50}$, which displays excellent antibacterial selectivity with a selectivity index of 80 and 16 for HC_5/MIC and IC_{50}/MIC, respectively (Fig. 2, I and J).

Antibacterial activity on clinically isolated pathogens, low toxicity, and insusceptibility to antimicrobial resistance of $\beta Lys_{50}HG_{50}$

We continued to examine the optimal poly-β-peptide, $\beta Lys_{50}HG_{50}$, for its activity against another eight strains of *S. aureus*, five of which are MRSA. $\beta Lys_{50}HG_{50}$ was active against all these strains and exert as a bactericidal agent, with MIC and minimum bactericidal concentration (MBC) identical, at 25 μg/ml in most cases (Fig. 3A). The antibacterial activity of the optimal poly-β-peptide, $\beta Lys_{50}HG_{50}$, was close to that of both the heterochiral poly-β-lysine and helical poly-β-L-lysine with MIC of 12.5 μg/ml and MBC of 12.5 to 25 μg/ml (fig. S28), which demonstrated that

introducing β-homo-glycine into poly-β-lysine with a suitable proportion can retain the antibacterial activity.

We also evaluated the toxicity of $\beta Lys_{50}HG_{50}$, poly-β-lysine, and helical poly-β-L-lysine on multiple mammalian cells, including sources from murine, rabbit, primate, and human. $\beta Lys_{50}HG_{50}$ showed low toxicity on all these mammalian cells with IC_{50} of 200 to 400 μg/ml; in sharp contrast, poly-β-lysine and the helical poly-β-L-lysine were quite toxic to all these mammalian cells with IC_{50} of 12.5 to 50 μg/ml (Fig. 3B and fig. S29), which highlights the importance and effectiveness of introducing β-homo-glycine into poly-β-lysine to effectively reduce the toxicity of resulting poly-β-peptides rather than reduce the toxicity of poly-β-peptides just by breaking the helicity.

In a further antibacterial resistance study, we found that treating *S. aureus* with $\beta Lys_{50}HG_{50}$ continuously at 0.5 × MBC for 483 generations ($\beta Lys_{50}HG_{50}$-P_{483}) did not induce the bacteria to develop resistance; in sharp contrast, treating *S. aureus* with ciprofloxacin continuously at 0.5 × MBC induced the bacteria to develop 250-fold resistance already after 480 generations (siprofloxacin-P_{480}) (Fig. 3C and figs. S30 and S31). In addition, we analyzed the final generation of *S. aureus* from the above $\beta Lys_{50}HG_{50}$ and ciprofloxacin treatment for their possible cross-resistance to other antibiotics. In contrast, the final generation of *S. aureus* from $\beta Lys_{50}HG_{50}$ treatment showed no cross-resistance to all eight antibiotics, whereas the final generation of *S. aureus* from ciprofloxacin treatment showed strong cross-resistance to levofloxacin, moxifloxacin, and norfloxacin, respectively, for 62.5-, 20-, and 128-fold changes on MIC
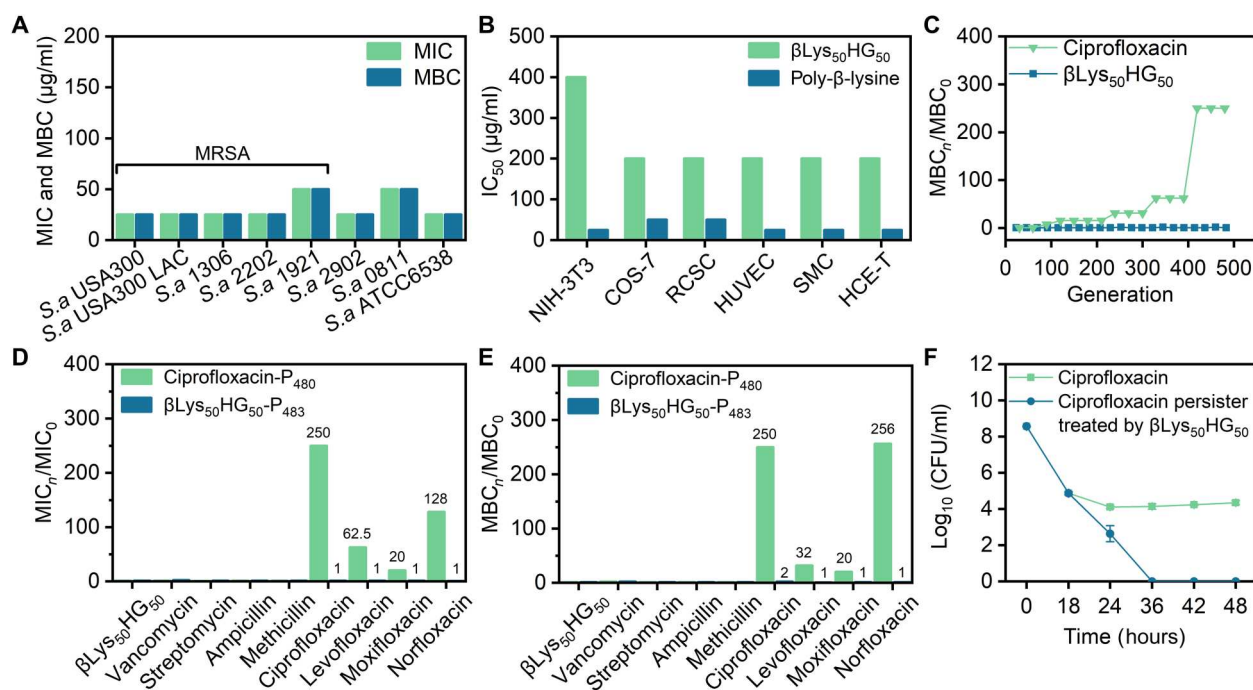

Fig. 3. $\beta Lys_{50}HG_{50}$ displayed powerful activity, nontoxicity, insusceptibility to antibacterial resistance, and effective activity on persister cells. (**A**) Antibacterial activity of $\beta Lys_{50}HG_{50}$ against a variety of *S. aureus*, including five strains of MRSA. (**B**) Cytotoxicity of $\beta Lys_{50}HG_{50}$ to a variety of cells from different tissue sources, including mouse embryo fibroblast cells (NIH-3T3), African *Chlorocebus sabaeus* kidney fibroblast cells (COS-7), rabbit corneal stroma cells (RCSC), human umbilical vein endothelial cells (HUVEC), human aortic smooth muscle cells (SMC), and human corneal epithelium cells (HCE-T). (**C**) Antibacterial resistance test of $\beta Lys_{50}HG_{50}$ and ciprofloxacin against *S. aureus* 6538 at a concentration of 0.5 × MBC. (**D** and **E**) MIC and MBC of various antibiotics to *S. aureus* 6538 ($\beta Lys_{50}HG_{50}$-P_{483} and ciprofloxacin-P_{480}), which was obtained by treating with $\beta Lys_{50}HG_{50}$ and ciprofloxacin continuously at 0.5 × MBC for 483 and 480 generations, respectively. (**F**) Killing kinetics of persister cells (obtained by treating with ciprofloxacin at 10 × MIC) with ciprofloxacin and $\beta Lys_{50}HG_{50}$ at a concentration of 8 × MIC. Data are presented as means ± SD.

(Fig. 3D) and 32-, 20-, and 256-fold changes on MBC (Fig. 3E). Moreover, we found that 8 × MIC concentration of βLys$_{50}$HG$_{50}$ effectively killed all [with 8.5-log colony-forming unit (CFU) reduction] MRSA persister cells (45), which are highly resistant to most antibiotics, such as ciprofloxacin in our study (Fig. 3F). The time-killing kinetics showed that βLys$_{50}$HG$_{50}$ killed more than 99% of *S. aureus* in 4 hours at a concentration of 2 × MIC, which was similar to streptomycin (fig. S32).

Bacterial membrane–penetrating mechanism of βLys$_{50}$HG$_{50}$

The superior antibacterial performance of the optimal poly-β-peptide βLys$_{50}$HG$_{50}$ encouraged us to explore its antibacterial mechanism using the blue fluorescent probe 7-diethylamino-3-(4-maleimidophenyl)-4-methylcoumarin–conjugated poly-β-peptides (fig. S21). Using a laser scanning confocal microscopy (LSCM) to study *S. aureus* incubated with Dye-βLys$_{50}$HG$_{50}$ and propidium iodide (PI), we observed that Dye-βLys$_{50}$HG$_{50}$ started to enrich inside bacterial cells almost immediately after incubation, without obvious enrichment on the bacterial membrane first, which implies that Dye-βLys$_{50}$HG$_{50}$ has a weak interaction with bacterial membrane and cross the membrane easily to enrich inside bacteria (Fig. 4, A and B). No observable PI signal was found within *S. aureus* cells until incubation over 410 s, and then a quick uptake of PI was observed, indicating that the bacteria were dead and the membrane was disrupted (Fig. 4, A and B). To verify that βLys$_{50}$HG$_{50}$ can cross the cytomembrane and enrich inside bacteria, we used a membrane-impermeable fluorescence quencher trypan blue to quench the fluorescence from extracellular Dye-βLys$_{50}$HG$_{50}$. The result of LSCM showed that fluorescence intensity has no obvious decrease after addition of trypan blue, which indicates that Dye-polypeptide crosses the membrane and enriches in the cytosol but not in the membrane (fig. S34). This result is consistent with the conclusion in the above LSCM analysis. We continued to conduct the membrane depolarization analysis using 3,3′-dipropylthiadicarbocyanine iodide [diSC$_3$(5)] dye as the membrane potential indicator and found that βLys$_{50}$HG$_{50}$ induces an almost negligible change in membrane potential even at 5 × MIC concentration (Fig. 4C), an observation consistent to weak βLys$_{50}$HG$_{50}$-membrane interaction in the above LSCM analysis.

For comparison, we also studied the antibacterial mechanism of the heterochiral poly-β-lysine and helical poly-β-L-lysine. LSCM analysis using dye-conjugated polypeptides showed that the heterochiral poly-β-lysine performs similarly to the optimal poly-β-peptide βLys$_{50}$HG$_{50}$ and enriches inside bacterial cells almost immediately after incubation (fig. S33, A and B), which is distinct from the performance of the helical poly-β-L-lysine that almost disrupts the membrane directly without the need to enter the bacteria first (fig. S33, C and D). This result supported our design to switch the antibacterial mechanism of polypeptides by breaking the helical structure. A continuous membrane depolarization analysis echoed the above conclusion in mechanism switching by breaking the helical structure of polypeptides (fig. S33E).

βLys$_{50}$HG$_{50}$ shows strong DNA binding and ROS-related antibacterial mechanism

We then turn our attention to figuring out what may happen after βLys$_{50}$HG$_{50}$ entered into the bacteria. We found that βLys$_{50}$HG$_{50}$ has strong binding to DNA even at a low N/P ratio of 0.5 to 1

(Fig. 4D), which indicated a possible bacterial killing mechanism via interaction with DNA and by interfering with the transcription process (46–48). It is known that DNA binding may induce bacteria to have a spontaneous Save Our Souls (SOS) response and release a large amount of ROS (49–51), which in turn may damage the cell membrane directly or result in bacterial apoptosis (52–54). To examine these possibilities, we analyzed the intracellular ROS level after bacterial incubation with βLys$_{50}$HG$_{50}$, using 2′,7′-dichlorofluorescin diacetate (DCFH-DA) as a ROS probe. After incubating *S. aureus* with βLys$_{50}$HG$_{50}$ at 2 × MIC for 50 min, we observed a substantial increase (~6.0-fold increase) of intracellular ROS level (Fig. 4E). When 7.5 mM ROS quencher *N*-acetyl-L-cysteine (NAC) was used in the above study, we found that the intracellular ROS level of βLys$_{50}$HG$_{50}$-treated *S. aureus* is stabilized at a normal level as in the phosphate-buffered saline (PBS) control group (Fig. 4E), within which the antibacterial activity of βLys$_{50}$HG$_{50}$ is lost (Fig. 4F). These studies indicate that the intensive increase of intracellular ROS level and ROS-associated cell damage is highly possible to play a vital role in the complex antibacterial mechanism of poly-β-peptide. To further investigate this antibacterial mechanism, we conducted transmission electron microscopy (TEM) and scanning electron microscopy (SEM) characterizations toward βLys$_{50}$HG$_{50}$-treated and untreated *S. aureus*. In TEM characterization, we observed obvious bacterial membrane disruption and intracellular dark deposition that may be generated by the binding of poly-β-peptide to bacterial DNA (Fig. 4G). In SEM characterization, the bacterial membrane became wrinkled and concaved after βLys$_{50}$HG$_{50}$ and poly-β-lysine treatment (Fig. 4H); in sharp contrast, we observed the lysis of bacterial membrane after the helical poly-β-L-lysine treatment, which indicates the membrane damage mechanism (fig. S33F). In addition, we observed vesicles with a diameter of about 150 nm outside of the bacterial membrane, which could be generated by the SOS response after βLys$_{50}$HG$_{50}$ entered into the bacteria to interact with DNA (Fig. 4H) (55, 56). Overall, these TEM and SEM results are consistent with aforementioned observations in antibacterial mechanism study. We observed a similar antibacterial mechanism of poly-β-lysine, which penetrates the membrane and may bind with DNA to induce bacteria to have a spontaneous SOS response and release a large amount of ROS, which in turn may damage the cell membrane directly or result in bacterial apoptosis (figs. S33 and S35 to S38).

Evaluating the therapeutic potential in local infections using MRSA-infected full-thickness wound, keratitis, and neutropenic thigh infection models

Encouraged by the superior antibacterial activity as well as low hemolysis and cytotoxicity of βLys$_{50}$HG$_{50}$, we continued to evaluate the therapeutic potential of βLys$_{50}$HG$_{50}$ in three MRSA-infected animal models, covering both local and systemic infections (Figs. 5 and 6). In the full-thickness wound model, wounds infected with MRSA were treated topically with βLys$_{50}$HG$_{50}$ and vancomycin (the positive control), respectively, at 24 hours after infection (Fig. 5A). βLys$_{50}$HG$_{50}$ treatment resulted in a substantial reduction of bacterial load in the infected issue (a 3.1-log CFU reduction relative to the saline-treated group), which is even better than the performance of vancomycin showing a 2.0-log CFU reduction (Fig. 5B). Moreover, histological analysis by hematoxylin and eosin (H&E) staining of the wounds showed a strong inflammatory infiltration in the saline-treated group but negligible inflammatory
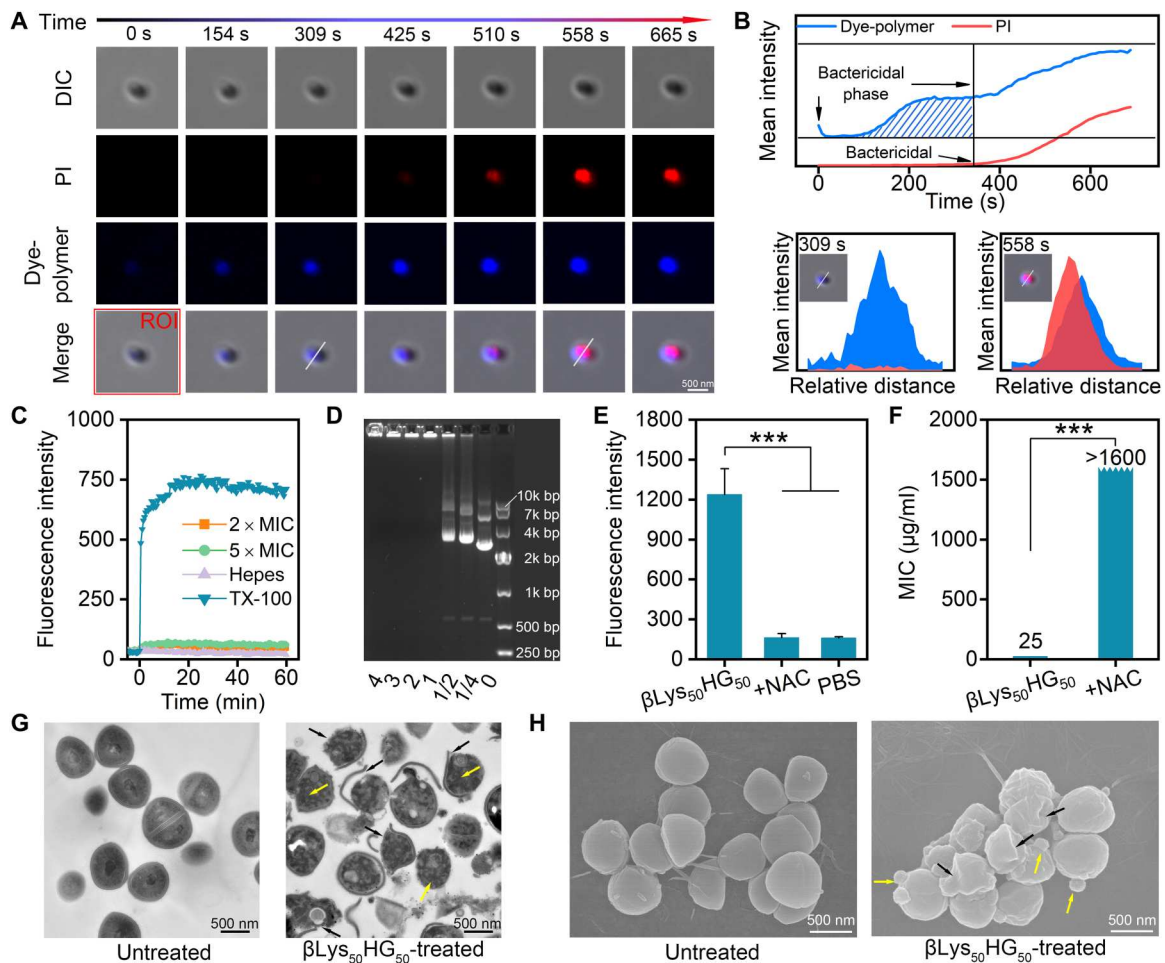
Fig. 4. Antibacterial mechanism of βLys$_{50}$HG$_{50}$. (**A**) Time-lapse imaging of the interaction between βLys$_{50}$HG$_{50}$ and bacteria by laser scanning confocal microscopy at a concentration of 2 × MIC, with the presence of propidium iodide (PI). (**B**) Overall fluorescence curve and fluorescence distribution curve in region of interest. (**C**) *S. aureus* cytoplasmic membrane depolarization induced by βLys$_{50}$HG$_{50}$ at a concentration of 2 × MIC and 5 × MIC concentration. Hepes solution [5 mM Hepes (pH 7.4) and 20 mM glucose] was used as a blank, and Triton X-100 (1‰ in Hepes solution) was used as a positive control. (**D**) Determination of the electrophoretic rate of plasmid DNA after mixing with βLys$_{50}$HG$_{50}$ at different ratios of N/P (βLys$_{50}$HG$_{50}$/DNA). (**E**) Intracellular ROS fluorescence produced by *S. aureus* treated with PBS buffer, βLys$_{50}$HG$_{50}$ (2 × MIC), and the mixture of βLys$_{50}$HG$_{50}$ (2 × MIC) and NAC (7.5 mM) in the presence of 2′,7′-dichlorofluorescin diacetate (DCFH-DA). (**F**) MIC value of βLys$_{50}$HG$_{50}$ against *S. aureus* in the presence or absence of NAC (7.5 mM), which can inhibit the intracellular ROS. (**G**) TEM characterization of *S. aureus* with and without βLys$_{50}$HG$_{50}$ treatment at 2 × MIC concentration; yellow arrows indicate the intracellular dark deposits, and black arrows indicate a damage of the integrity of the bacteria. (**H**) SEM characterization of *S. aureus* with and without βLys$_{50}$HG$_{50}$ treatment at 2 × MIC concentration; yellow arrows indicate extracellular vesicles, and black arrows indicate the wrinkles and concaves of the bacteria membrane. Data are presented as means ± SD. Statistical analysis, two-tailed *t* test, ***$P < 0.001$.

infiltration in the βLys$_{50}$HG$_{50}$ and vancomycin group (Fig. 5C). In the MRSA infection keratitis model, mice were treated with topical eye drop solutions containing βLys$_{50}$HG$_{50}$ and vancomycin (the positive control), respectively, at 14 hours after infection (Fig. 5D). βLys$_{50}$HG$_{50}$ treatment resulted in a substantial reduction of bacterial load in the infected cornea (a 2.9-log CFU reduction relative to the saline-treated group), which is better than the performance of vancomycin showing a 1.3-log CFU reduction (Fig. 5E). Moreover, histological analysis by H&E staining of the cornea showed a strong inflammatory infiltration in the saline-treated group but negligible inflammatory infiltration in the βLys$_{50}$HG$_{50}$ and vancomycin group (Fig. 5F). In addition, histological analysis showed nontoxicity to the corneas of noninfected mice (fig. S39). In the neutropenic thigh infection model, thighs infected with MRSA by intramuscular injection for 2 hours were treated subcutaneously

with saline, βLys$_{50}$HG$_{50}$, and vancomycin, respectively (Fig. 5G). After the treatment, bacterial load analysis showed that βLys$_{50}$HG$_{50}$ is as effective as vancomycin in remarkably reducing the bacterial load for around 3.0- and 4.0-log CFU compared to the saline treatment group (Fig. 5H). The histological morphology by Gram staining of the thigh tissues showed that βLys$_{50}$HG$_{50}$ and vancomycin treatment resulted in a substantial *S. aureus* load reduction compared with saline-treated thigh (Fig. 5I), indicating that βLys$_{50}$HG$_{50}$ effectively alleviated the severity of thigh infection, as did vancomycin.

Evaluating the therapeutic potential in MRSA lung infection and systemic peritonitis models
We continued to evaluate the therapeutic potential of βLys$_{50}$HG$_{50}$ in even more challenging MRSA lung infection and systemic
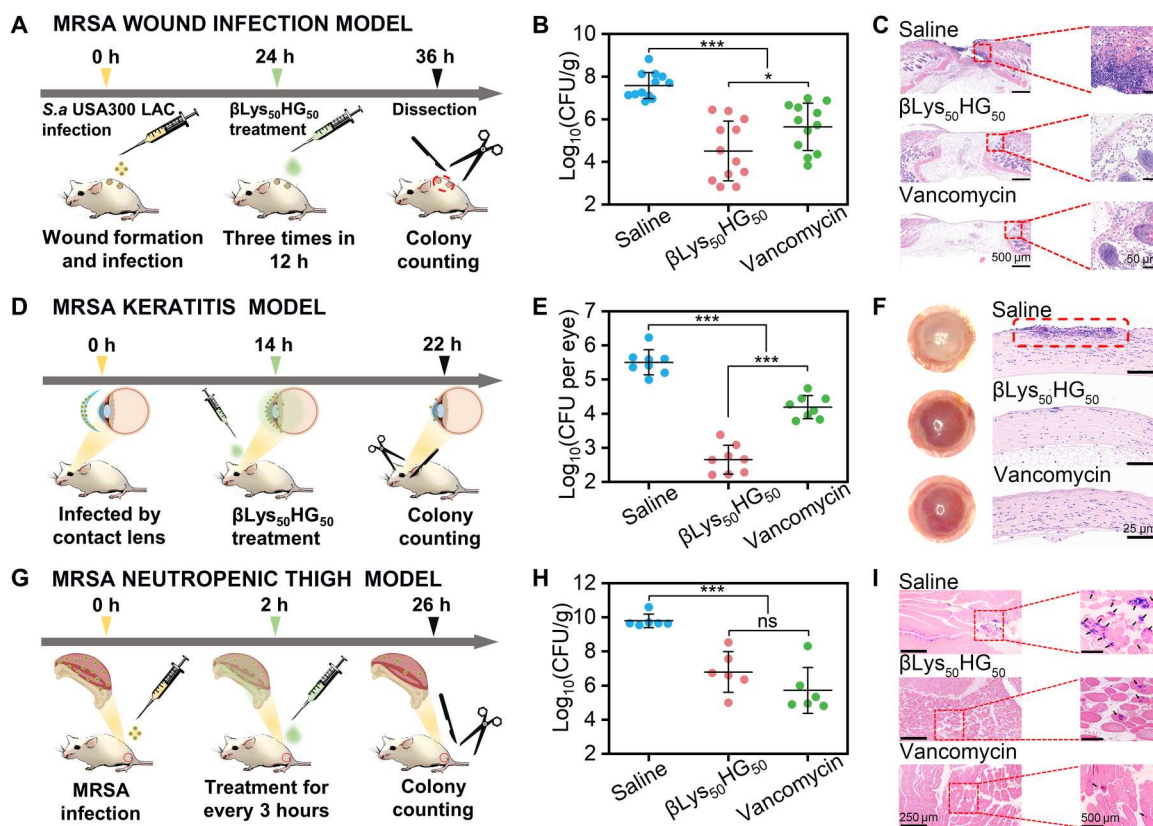
Fig. 5. Evaluating the in vivo therapeutic potential of $\beta Lys_{50}HG_{50}$ using MRSA wound infection, keratitis, and neutropenic thigh infection models. (A) In the full-thickness wound infection model, bacterial suspension (2.5×10^5 CFU/ml, 10 μl) was applied to the wound ($n = 6$ mice per group) and infected for 24 hours followed by topical treatments with saline, $\beta Lys_{50}HG_{50}$ (5 mg/ml), or vancomycin (5 mg/ml), and bacterial loading analysis was conducted after the treatment at 36 hours after infection. **(B)** Bacterial loading analysis and **(C)** wound histological analysis of mice after treatments. **(D)** In the keratitis model, the contact lenses that were incubated in bacterial suspension for 18 hours were placed on the injured cornea ($n = 4$ mice per group) and infected for 14 hours followed by topical treatments with saline, $\beta Lys_{50}HG_{50}$, or vancomycin at a concentration of $400 \times$ MIC, and bacterial loading analysis was conducted after the treatment. **(E)** Bacterial loading analysis and **(F)** wound histological analysis of the eyeball after treatments. **(G)** In the MRSA neutropenic thigh infection model, bacterial suspension (3.3×10^6 CFU/ml, 30 μl) was intramuscularly injected into the right thigh ($n = 6$ mice per group) and infected for 2 hours followed by subcutaneous treatments with saline, $\beta Lys_{50}HG_{50}$ (5 mg/ml), or vancomycin (5 mg/ml). Bacterial loading analysis was conducted after the treatment at 26 hours after infection. **(H)** Bacterial loading analysis and **(I)** thigh tissue histological analysis by Gram staining after treatment; black arrows represent the bacteria distribution. Data are represented as means ± SD. Statistical analysis, two-tailed t test, *$P < 0.05$; ***$P < 0.001$. ns (not significant), $P > 0.05$.

peritonitis mice models (Fig. 6). In the lung infection model, mice were infected with MRSA by intratracheal instillation at a lethal dose in the survival experiment, with all untreated mice dying within 24 hours (Fig. 6A). Notably, five of six mice survived after intratracheal treatment of $\beta Lys_{50}HG_{50}$, which is as effective as vancomycin treatment (five of six mice survived) at the same dose (Fig. 6B). This result indicated that $\beta Lys_{50}HG_{50}$ has strong therapeutic potential in treating MRSA lung infection. Bacterial load analysis showed that $\beta Lys_{50}HG_{50}$ is as effective as vancomycin in remarkably reducing the bacterial load for around 2.3- and 1.9-log CFU, respectively, compared to the saline treatment group in the lung (Fig. 6C). We also examined the histological morphology by H&E staining of lung and found that infection caused severe lesions of lung in the saline-treated group with bronchus epithelial damage, epithelial sloughing, severe bronchitis, and alveolar hemorrhage (Fig. 6D) compared to the group without any treatment (fig. S40). After treatment with either $\beta Lys_{50}HG_{50}$ or vancomycin, tissue lesions caused by bacterial infection are effectively relieved.

In the systemic peritonitis models, mice were infected by intraperitoneal injection of MRSA at a lethal dose in the survival experiment (Fig. 6E), and five of six untreated mice died within 24 hours. Notably, all the mice survived after intraperitoneal administration of a single dose of $\beta Lys_{50}HG_{50}$ at 40 mg/kg, which surpassed the performance (five of six mice survived) of vancomycin treatment at the same dose (Fig. 6F). This result indicates that $\beta Lys_{50}HG_{50}$ has strong therapeutic potential in treating systemic MRSA infections. In addition, after mice were infected over 0.5 hour, we analyzed the bacterial load in five major organs (57–59), bloodstream, and peritoneal fluid of mice. We found bacterial load at over 6-log CFU/g tissue in most organs, indicating a severe infection in mice already (Fig. 6G, the control). After antibacterial treatment for 48 hours, bacterial load analysis showed that $\beta Lys_{50}HG_{50}$ is as effective as vancomycin in remarkably reducing the bacterial load for around 2.5- to 4-log CFU compared to the saline treatment group, in all five organs, bloodstream, and peritoneal fluid of mice (Fig. 6G). We also examined the histological morphology by H&E staining of major organs and found that infection caused
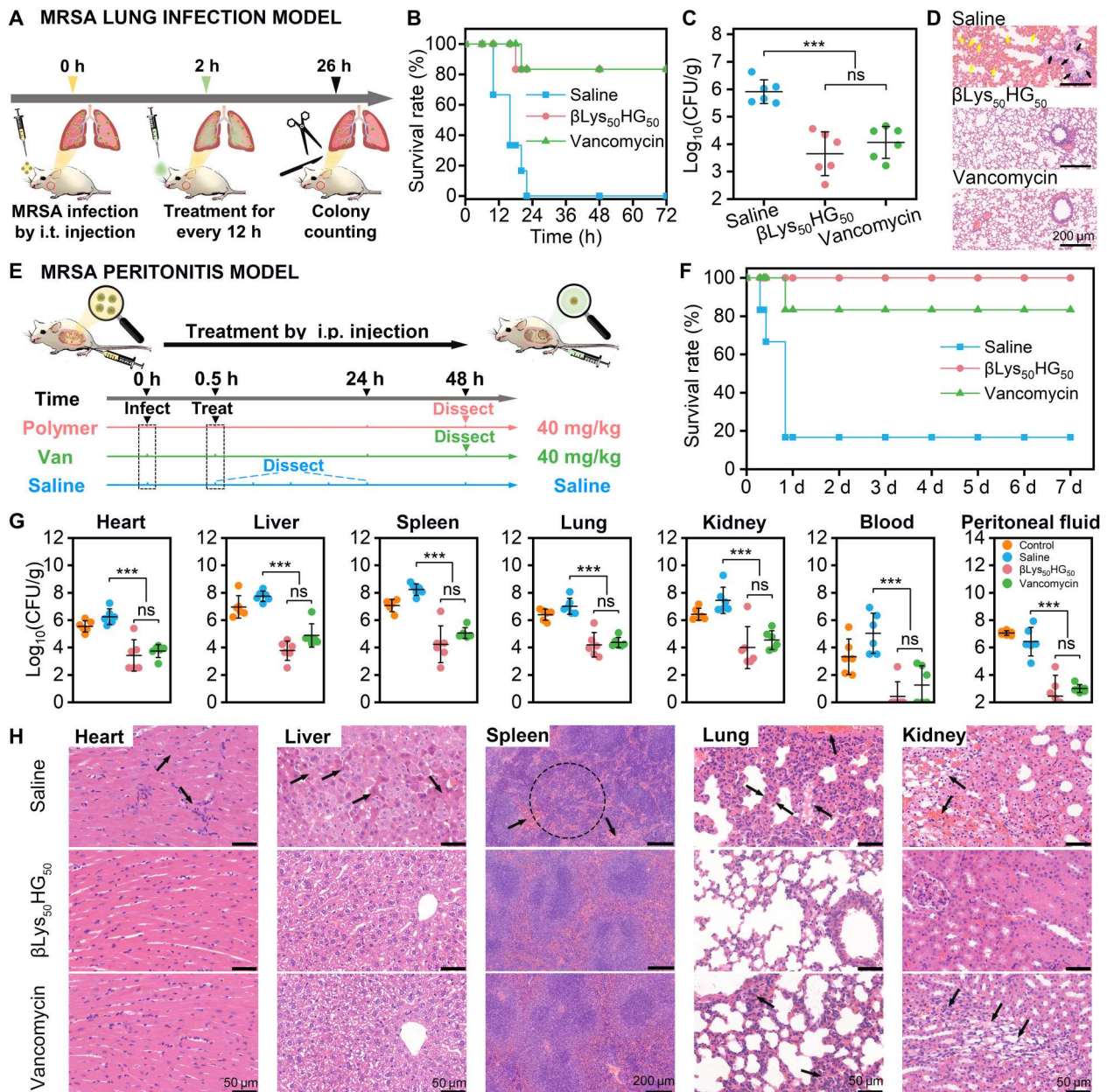
Fig. 6. Evaluating the in vivo therapeutic potential of βLys₅₀HG₅₀ by challenging MRSA lung infection and systemic peritonitis models. (**A**) In the lung infection model, bacterial suspension (5×10^7 CFU/ml, 30 μl) was intratracheally (i.t.) instilled to the lung ($n = 6$ mice per group) and infected for 2 hours followed by nebulizing treatments intratracheally with saline, βLys₅₀HG₅₀ (5 mg/ml), or vancomycin (5 mg/ml). Bacterial loading analysis was conducted after the treatment at 26 hours after infection. (**B**) Survival rates of the MRSA-infected mice after the treatments with saline, βLys₅₀HG₅₀, or vancomycin within 72 hours. (**C**) Bacterial loading analysis and (**D**) lung histological analysis by H&E staining of mice after treatment, with black arrows and yellow arrows representing histological anomalies in bronchus and alveoli, respectively. (**E**) In the mouse peritonitis model, MRSA-infected mice were prepared by intraperitoneal (i.p.) injection of bacterial suspension (1.5×10^9 CFU/ml, 200 μl) for 0.5 hour ($n = 6$ mice per group), followed by intraperitoneal treatments with saline, βLys₅₀HG₅₀ (40 mg/kg), or vancomycin (40 mg/kg). The bacterial loading was analyzed after antibacterial treatment for 48 hours. (**F**) Survival rates of the MRSA-infected mice after the treatment with saline, βLys₅₀HG₅₀, or vancomycin in 7 days. (**G**) Bacterial loading analysis of different organs, blood, and peritoneal fluid after the treatment. (**H**) Histological analysis by H&E staining of different organ sections from the mice after the treatment with saline, βLys₅₀HG₅₀, and vancomycin; black arrows represent histological anomalies. Data are represented as means ± SD. Statistical analysis, two-tailed t test, ***$P < 0.001$. ns (not significant), $P > 0.05$.

various organ lesions in the saline-treated group (Fig. 6H) compared to the group with normal feeding and without any treatment (fig. S40). We observed red staining of the partial hepatocyte necrosis, disappearance of the normal splenic white pulp structure, thickening of the alveolar wall and aggregation of inflammatory cells, hemorrhaging around proximal renal tubular, and degeneration of the proximal renal tubular epithelial cell. After treatment with either $\beta Lys_{50}HG_{50}$ or vancomycin, tissue lesions caused by bacterial infection are effectively relieved. It is worth mentioning that histological analysis of the kidney after vancomycin treatment showed lesions in the proximal renal tubules, which may be the nephrotoxicity of vancomycin (60, 61).

In vivo toxicity evaluation of $\beta Lys_{50}HG_{50}$

In addition to the above therapeutic effectiveness studies, we also evaluated the in vivo toxicity of the optimal poly-β-peptide $\beta Lys_{50}HG_{50}$ because even some classical antibiotics, such as vancomycin, are known to have nephrotoxicity (60, 61). One-time injection of $\beta Lys_{50}HG_{50}$ and poly-β-lysine in the tail vein was conducted with the maximum dose that mice can receive in a single administration, which enables us to assess the acute toxicity of poly-β-peptides. When the injection concentration reached 12.5 mg/kg, all the mice in the poly-β-lysine group showed sluggish behavior

immediately after administration, and all died within 30 to 60 min (Fig. 7A), preventing us from monitoring the behavior, body weight, and physiological indicators of these mice. Notably, after injection of $\beta Lys_{50}HG_{50}$ at a concentration of 40 mg/kg, we did not observe any differences on mice compared to the saline group within 14 days, including murine behavior, survival rate (Fig. 7A), body weight (Fig. 7B), blood biochemical indices (Fig. 7, C to I), as well as liver and kidney histological analysis by H&E staining (Fig. 7, J and K). The normal levels of alanine aminotransferase (ALT) and aspartate aminotransferase (AST) in the $\beta Lys_{50}HG_{50}$-treated mice indicated the lack of liver toxicity. The normal levels of blood urea nitrogen (BUN) and serum creatinine (CREA) in the $\beta Lys_{50}HG_{50}$-treated mice indicated a lack of nephrotoxicity. The normal levels of sodium (Na^+), potassium (K^+), and chloride (Cl^-) in the $\beta Lys_{50}HG_{50}$-treated mice indicated no electrolyte disturbance in vivo. All these results indicated that the optimal poly-β-peptide $\beta Lys_{50}HG_{50}$ has low toxicity in vivo and is effective and safe to use as a promising antibacterial agent.

DISCUSSION

To address the grand challenge of antibiotic-resistant bacterial infections, HDP-mimicking antibacterial peptides have been actively
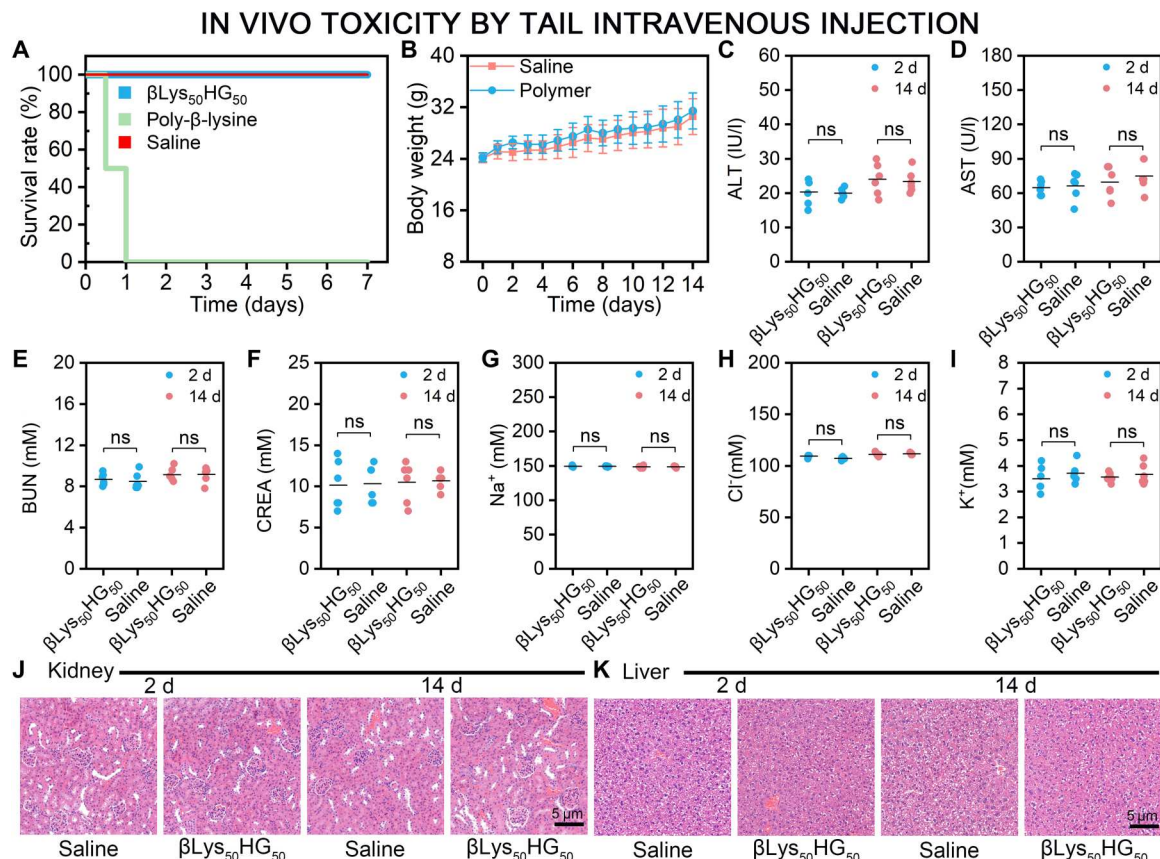

Fig. 7. In vivo toxicity study of poly-β-peptide in mice. (**A**) Survival rates of the mice in 7 days ($n = 6$ mice per group) after the single dose of intravenous injection with saline, $\beta Lys_{50}HG_{50}$ (40 mg/kg), or poly-β-lysine (12.5 mg/kg). (**B**) Body weight of normally housed mice after a single dose of intravenous injection for 14 days. (**C** to **I**) Blood biochemical indices (ALT, AST, BUN, CREA, Na^+, Cl^-, and K^+) of the mice at 2 and 14 days after the single dose of intravenous injection with saline or $\beta Lys_{50}HG_{50}$ (40 mg/kg). (**J** and **K**) H&E staining of kidney and liver sections from the mice at 2 and 14 days after the single dose of intravenous injection with saline or $\beta Lys_{50}HG_{50}$ (40 mg/kg). Data are presented as means ± SD. Statistical analysis, two-tailed t test. ns (not significant), $P > 0.05$.

studied. Among these antibacterial peptides, poly-β-L-lysine is known to have potent antibacterial activity but high cytotoxicity that is caused by the α-helical structure, which has strong interaction with cell membrane. Here, we report a strategy to develop low-toxic poly-β-peptides by breaking the helical structure of poly-β-L-lysine using racemic lysine residue to reduce interaction of polypeptide with cell membrane and further introducing β-homo-glycine residue into poly-β-peptides to reduce charge density and, therefore, reduce cytotoxicity. The optimal poly-β-peptide βLys$_{50}$HG$_{50}$ displays effective antibacterial activity on clinically isolated drug-resistant *S. aureus*, including MRSA, and can also eliminate MRSA persister cells efficiently and completely. Moreover, βLys$_{50}$HG$_{50}$ shows potent therapeutic potential for both local and systemic infections in MRSA-infected murine full-thickness wound model, keratitis model, and peritonitis model. βLys$_{50}$HG$_{50}$ shows low toxicity both in vitro and in vivo, suggesting excellent biosafety in clinical application. In addition, *S. aureus* does not acquire antimicrobial resistance even after bacteria are treated with βLys$_{50}$HG$_{50}$ continuously at 0.5 × MBC over 483 generations, which is ascribed to the DNA binding and intracellular ROS level increase–related bactericidal mechanism of βLys$_{50}$HG$_{50}$. These results demonstrate that our strategy in designing potent and low toxic poly-β-peptides is effective and that the optimal poly-β-peptide βLys$_{50}$HG$_{50}$ has potent antibacterial activity, excellent biosafety, and strong therapeutic potential in treating drug-resistant bacterial infections. Moreover, the easy synthesis and structural diversity of poly-β-peptides imply great potential of βLys$_{50}$HG$_{50}$ as a promising antibacterial agent in clinical application. Although this strategy may not be generalizable to all the extensive and complicated chemical structures of peptides, peptoids, and other synthetic mimics, it can inspire the design and discovery of antimicrobials against drug-resistant pathogens. Further investigations are worth conducting to explore the generalizability of this strategy.

MATERIALS AND METHODS

Hemolysis test
Fresh human blood was used for the hemolysis test, which was diluted with tris-buffered saline (TBS; pH 7.2) and centrifuged at 3700 rpm for 5 min. hRBCs were collected after washing for three times and diluted to a working concentration of 5% (v/v) with TBS. Poly-β-peptide was serially diluted twofold into 96-well plates, and the prepared hRBC suspension was added to each well of the 96-well plate in equal volume and mixed with the poly-β-peptide solution. The final concentration of poly-β-peptide ranged from 15.6 to 2000 μg/ml. hRBCs in TBS without poly-β-peptide were used as the blank, and hRBCs in Triton X-100 (1‰ in TBS solution) were used as the control. The plate was incubated in a constant temperature incubator at 37°C for 1 hour, and the optical density (OD) value of each well was measured under 405 nm. The percentage of hemolysis was calculated by the following formula. The experiment was performed three times independently.

$$\% \text{ hemolysis} = \frac{V_{405}^{\text{peptide}} - V_{405}^{\text{blank}}}{V_{405}^{\text{control}} - V_{405}^{\text{blank}}} \times 100 \tag{1}$$

(V_{405}^{peptide} represents the OD value of hRBCs that were treated with poly-β-peptide. V_{405}^{control} represents the OD value of the hRBCs that were treated with Triton X-100. V_{405}^{blank} represents the OD value of TBS solution.) All experiments have been approved by the ethics committee of Tenth People's Hospital, Shanghai Tongji University. The guiding principles for collecting and using of hRBC are provided by Tenth People's Hospital, Shanghai Tongji University. The research was informed and consented by the donor.

Cytotoxicity test
Mammalian cells, such as the mouse embryonic fibroblast cells (NIH-3T3), were cultured in tissue culture polystyrene dishes using Dulbecco's modified Eagle's medium (DMEM), which was supplemented with 10% fetal bovine serum, penicillin (100 U/ml), and streptomycin (100 μg/ml), at the conditions of 5% CO$_2$ and 37°C. The cells were trypsinized and diluted to a working concentration of 5×10^4 cells/ml. Then, 100 μl of the suspension was added to each well of a 96-well plate, and the plate was incubated overnight. The culture medium was replaced by fresh medium with poly-β-peptide, which was twofold serially diluted at the final concentration range of 6.25 to 200 μg/ml, and the plate was incubated for 24 hours. Ten microliters of 3-(4,5-dimethylthiazol-2-yl)-2,5-diphenyltetrazolium bromide (MTT) solution (5 mg/ml in PBS) was added to each well, and the plate was incubated in the dark for 4 hours. After removing the medium, 150 μl of dimethyl sulfoxide (DMSO) was added to each well and shaken gently for 15 min. Wells with DMSO only were used as the blank, and wells of cells cultured without peptide treatment were used as the control. The OD value of each well was measured with a SpectraMax M2 microplate reader at 570 nm, and the percentage of cytotoxicity was calculated by the following formula. The experiment was performed three times independently.

$$\% \text{ cell viability} = \frac{V_{570}^{\text{peptide}} - V_{570}^{\text{blank}}}{V_{570}^{\text{control}} - V_{570}^{\text{blank}}} \times 100 \tag{2}$$

(V_{570}^{peptide} represents the OD value of wells that were cultured in DMEM with poly-β-peptide. V_{570}^{control} represents the OD value of the wells that were cultured in normal DMEM medium. V_{570}^{blank} represents the OD value of DMSO.)

MIC and MBC test
We conducted MIC experiments on different bacterial species to evaluate the antibacterial activity of this series of poly-β-peptides, and vancomycin was used as a control. The bacteria were dispersed in a high-temperature sterilized glass conical flask with Luria-Bertani (LB) medium and cultured at 37°C with continuous shaking for 10 hours. After centrifuging and washing with PBS, the bacterial suspension was diluted in Mueller-Hinton (MH) liquid medium to a concentration of 2×10^5 CFU/ml as a working suspension. The poly-β-peptide solution and antibiotics were added to each well of a 96-well plate in serial twofold dilutions in MH medium at a concentration ranging from 1.56 to 200 μg/ml, and an equal volume of the previously prepared bacterial suspension was mixed with the above solution. MH medium was used as the blank, and MH medium added with an equal amount of bacterial suspension was used as a control. The plate was incubated at 37°C for 9 hours, and the OD value of each well was measured with a SpectraMax M2 microplate reader at 600 nm. The percentage of bacterial cell growth in each well was calculated following the

formula

$$\% \text{ cell growth} = \frac{V_{600}^{\text{peptide}} - V_{600}^{\text{blank}}}{V_{600}^{\text{control}} - V_{600}^{\text{blank}}} \times 100 \qquad (3)$$

(V_{600}^{peptide} represents the OD value of wells that were treated with poly-β-peptide. V_{600}^{control} represents the OD value of wells that were cultured in normal MH medium. V_{600}^{blank} represents the OD value of MH medium.)

MBC value is defined as the lowest drug concentration that kills 99.9% of microorganisms. After the completion of the MIC experiment, 3 μl from each well of the abovementioned well plate was evenly spread onto LB agar, and the liquid was dried and incubated at 37°C for 14 hours. The values of MBC were obtained from the minimum concentration of nongrowing bacteria on LB agar plates, and each experiment was performed three times independently.

Antimicrobial resistance assessment
The method of antimicrobial resistance assessment has been modified slightly from the previously reported method (40). S. aureus ATCC6538 was cultured in LB medium at 37°C for 9 hours and diluted to 2×10^5 CFU/ml in 1 ml of MH medium containing βLys$_{50}$HG$_{50}$ (0.5 × MBC) or ciprofloxacin (0.5 × MBC), respectively. Then, the mixture was incubated at 37°C for 24 hours under shaking. An aliquot of 2.5 μl of the above mixture was diluted 400-fold in 1 ml of MH medium as a continuous drug stimulating cycle, containing the same concentration of βLys$_{50}$HG$_{50}$ or ciprofloxacin, respectively. The duration of each cycle is 24 hours, and the MIC and MBC of βLys$_{50}$HG$_{50}$ and ciprofloxacin against S. aureus ATCC6538 were examined for every four cycles. According to the obtained MBC value, the concentration of βLys$_{50}$HG$_{50}$ and ciprofloxacin should always be adjusted to 0.5 × MBC throughout the antimicrobial resistance study.

Bacteria growth kinetics
S. aureus ATCC6538, which was stimulated with poly-β-peptide or antibiotic for 8 days in antimicrobial resistance study, was cultured in LB medium at 37°C for 10 hours. The bacterial suspension was diluted to 2×10^6 CFU/ml in MH medium, which contained βLys$_{50}$HG$_{50}$ (0.5 × MBC) or ciprofloxacin (0.5 × MBC), respectively. Diluting aliquots of bacterial suspension were taken out at several time points and spread out on LB agar plates. After incubating at 37°C for 14 hours, the colonies were counted, and the growth rate of the bacteria was calculated followed by fitting the growth curve.

MRSA persister cell killing kinetics
S. aureus USA300 was used to study the bactericidal performance of βLys$_{50}$HG$_{50}$ to persistent MRSA cells. The cultivation operations of bacteria refer to the MIC experiment. The cultured log-phase S. aureus USA300 bacteria were diluted in MH medium to a final working suspension of 10^8 CFU/ml, which was challenged with ciprofloxacin at 10 × MIC. The mixture was incubated at 37°C for 18 hours under continuous shaking. Then, half of the mixture was centrifuged and washed by fresh MH medium to remove ciprofloxacin and treated with βLys$_{50}$HG$_{50}$ at 8 × MIC. As a control, the other half mixture was challenged with ciprofloxacin at 8 × MIC. Diluting aliquots of bacterial suspension were taken out at 24, 36, 42, and 48 hours and spread out on LB agar plates. These plates

were incubated at 37°C for 14 hours, and the number of colonies was counted to calculate the rate of persister cell killing.

Bactericidal kinetics
The bacterial working suspension (2×10^5 CFU/ml) was prepared according to the steps of the above MIC experiment, and then the working suspension was treated with βLys$_{50}$HG$_{50}$ and streptomycin at a concentration of 2 × MIC. The plate was incubated at 37°C, and diluted aliquots of bacterial suspension were taken out at several time points and spread out on LB agar plates. These plates were incubated at 37°C for 14 hours, and the number of colonies was counted to calculate and fit the bactericidal kinetics.

Time-lapse fluorescence confocal imaging
Dynamic microscopic imaging is used to study the process of poly-β-peptide–bacteria interactions. S. aureus 2904 was cultured in LB medium at 37°C for 6 hours and diluted in PBS to 10^7 CFU/ml as a working suspension. An aliquot of 10 μl of the above suspension was added to a glass-bottomed dish and stood for 5 min until the bacteria settled to the bottom of the dish. After finding a clear image of the bacteria, an aliquot of 10 μl of PBS, which contained Dye-βLys$_{50}$HG$_{50}$ (2 × MIC, blue fluorescence) and pyridinium iodide (10 μM, red fluorescence), was mixed slightly with the bacterial suspension. The interaction process was continuously recorded using a confocal microscope with three channels (bright field, emission wavelength of 455 and 617 nm).

Evaluation of polypeptide penetrating into bacteria
The trypan blue assay was conducted by following the previously published method with slight modifications (62, 63). S. aureus 2904 was cultured in LB medium at 37°C for 6 hours and diluted in PBS to 10^7 CFU/ml as a working suspension. Aliquots of bacterial suspension (1 ml) were prepared, and Dye-βLys$_{50}$HG$_{50}$ was added to the bacteria and incubated for 4 min at a concentration of 2 × MIC. S. aureus was collected and washed twice with PBS to remove the free Dye-βLys$_{50}$HG$_{50}$ in PBS. S. aureus was resuspended in 0.5 ml of PBS, and an aliquot of 0.5 ml of trypan blue solution was added. The mixture was incubated for 3 min at a final concentration of 1 mg/ml. S. aureus was collected and washed twice with PBS to remove trypan blue and resuspended in 0.5 ml of PBS. An aliquot of 10 μl of the above suspension was added to a glass-bottomed dish. The images were recorded using a confocal microscope with two channels (a bright-field channel and a blue channel with emission at 455 nm).

Depolarization experiment on cytoplasmic membrane
The membrane potential–sensitive fluorescent dye diSC$_3$(5) was used to measure the plasma membrane depolarization activity of poly-β-peptide. S. aureus was cultured at 37°C for 6 hours in LB medium, and then the bacteria were washed with Hepes solution [5 mM Hepes (pH 7.4) and 20 mM glucose] and diluted to give the working suspension at 10^7 CFU/ml. The bacterial suspension was incubated with 0.4 μM diSC$_3$(5) for 1 hour, and then potassium chloride was added to a final concentration of 0.1 M to balance the cytoplasmic and external K$^+$ concentration. An aliquot of 90 μl of the suspension was placed in a 384-well plate, and fluorescence intensity was recorded with a microplate reader (excitation $\lambda = 622$ nm, emission $\lambda = 673$ nm). Once fluorescence intensity was stable, an aliquot of 10 μl of the poly-β-peptide solution was

added to a final concentration of 2 × MIC and 5 × MIC. The changes of fluorescence intensity were recorded on a microplate reader continuously. Triton X-100 (1‰ in PBS) was used as a positive control. The experiment was performed three times independently.

ROS detection assay

The intracellular ROS level in *S. aureus* was detected by DCFH-DA, which is a ROS-sensitive fluorescent probe. Mid-logarithmic phase *S. aureus* was cultivated in LB medium at 37°C for 6 hours and incubated with 10 ml of DCFH-DA solution (20 μM in PBS) for 30 min at 37°C. *S. aureus* was collected and washed twice with PBS to remove DCFH-DA that was free in PBS and then diluted to 2×10^8 CFU/ml using PBS. An aliquot of 5 ml of bacterial suspension was added to an equal volume of NAC (15 mM in PBS) solution as a working suspension to a cell density of 10^8 CFU/ml, and the NAC concentration is 7.5 mM. An aliquot of 90 μl of working suspension was placed in a 384-well plate and incubated for 10 min; then, 10 μl of poly-β-peptide (40 × MIC) was added to a final poly-β-peptide concentration at 4 × MIC. The changes of fluorescence intensity were recorded continuously on a microplate reader, where the excitation wavelength is 488 nm and the emission wavelength is 530 nm. The test was independently repeated three times. The experiment was performed three times independently.

DNA binding test

DNA binding experiments are designed to investigate and conjecture the antibacterial mechanism. The method can refer to the previously published method (*40*). Poly-β-peptide and DNA were incubated for 15 min after calculating the number of amine groups (N) contained in the polypeptide and the number of phosphate anions (P) contained in the plasmid DNA backbone. The N/P ratio was set to 0.25:1, 0.5:1, 1:1, 2:1, 3:1, and 4:1, and then the DNA was precipitated by 2 μl of 6× SDS-free DNA loading buffer. The mixture was analyzed by electrophoresis using an agarose gel containing 1% NA-Red (the main component is ethidium bromide). A DNA marker from Sangon Biotech (order no. B600022) with a molecular weight of 250 to 10,000 base pairs (bp) was used as a reference. DNA bands were observed by gel visualization instruments and software imaging systems (ChampGel 5000 Plus, Sage Creation).

TEM characterization

S. aureus 2904 was cultured for 10 hours at 37°C in LB medium and diluted to 2×10^7 CFU/ml in MH medium for 25 ml as the working suspension. An aliquot of 25 ml of the βLys$_{50}$HG$_{50}$ (2 × MIC) MH solution was prepared and mixed with an equal volume of bacterial suspension in a 50-ml sterile Eppendorf tube and incubated at 37°C for 2.5 hours. An untreated bacterial suspension with the same concentration was used as a control. All the suspension was collected and centrifuged at 4000 rpm for 5 min and washed with PBS for three times. The collected bacteria were mixed with glutaraldehyde solution (2.5% in PBS) and fixed at 4°C overnight. The fixed buffer was removed by centrifugation, and then the bacteria were collected and washed with PBS, which were fixed with 1% osmium acid solution for 1 hour again. After removing the osmium acid solution, the bacteria were washed with PBS for three times and dehydrated by gradient concentration of ethanol solution (50, 60, 70, 80, 90, 95, and 100%). Subsequently, the bacteria were treated with acetone for 20 min, a mixture of acetone and embedding agent (v/v = 1:1) for

1 hour, and a mixture of acetone and embedding agent (v/v = 1:3) for 3 hours. After permeabilization, the bacteria were embedded overnight at 70°C. The embedded samples were sectioned using a Leica EM UC7 ultrathin sectioning machine to obtain 50-nm sections. The above sections were stained with lead citrate solution and uranium dioxide acetate solution for 10 min, followed by observation with TEM.

SEM characterization

S. aureus 2904 was cultured for 10 hours at 37°C in LB medium and diluted to 2×10^7 CFU/ml in MH medium for 1 ml as the working suspension. An aliquot of 1 ml of the poly-β-peptide MH solution (2 × MIC) was prepared and mixed with an equal volume of bacterial suspension in an Eppendorf tube and incubated at 37°C for 2.5 hours. The untreated bacterial suspension with the same concentration was used as a control. All the suspension was collected and centrifuged at 4000 rpm for 5 min and washed with PBS for three times. The collected bacteria were mixed with glutaraldehyde solution (2.5% in PBS) and fixed at 4°C overnight. After removing the fixed buffer, the bacteria were washed with PBS for three times and dehydrated by gradient concentration of ethanol solution (50, 60, 70, 80, 90, 95, and 100%). The samples were resuspended using 50 μl of 100% ethanol and dried under air for 12 hours after the samples containing ethanol were carefully added dropwise to the gold-plated sheet, followed by observation with SEM.

Murine full-thickness wound infection model

During animal experiments, all animal husbandry procedures and surgical operations are in accordance with the Guidelines for the Care and Use of Laboratory Animals of the Tenth People's Hospital, Shanghai Tongji University (license number, SYXK-2021-0012). All animal experiments were approved by the Animal Ethics Committee of the Tenth People's Hospital, Shanghai Tongji University (accreditation number of the laboratory, SHDSYY-2021-1729). The laboratory animal usage license is certified by Science and Technology Commission of Shanghai Municipality.

The infection model was conducted by following the previously published method (*64, 65*). *S. aureus* USA300 LAC was cultured in LB medium at 37°C for 10 hours and washed three times with saline after removing the medium and resuspending in saline for use. Eighteen female Institute of Cancer Research (ICR) mice (20 to 23 g) were used in the MRSA-infected full-thickness model. Mice were anesthetized by intraperitoneal injection of pentobarbital sodium at a single dose of 75 mg/kg. Hair was removed from the back of the anesthetized mice, and then the skin was disinfected with iodophor. An aliquot of 10 μl of *S. aureus* USA300 LAC (2.5×10^5 CFU/ml) suspension was dropped into the wound on both sides of the back, which were punctured with a 6-mm-diameter biopsy punch, and then the wound was covered with Tegaderm dressing (3M, St Paul, MN) to avoid contamination. After 24 hours of preinfection, these mice were divided into three groups randomly and treated with different solutions: saline (placebo, negative control), βLys$_{50}$HG$_{50}$ (5 mg/ml), and vancomycin (5 mg/ml, positive control), which were applied every 4 hours for three times. Four hours after the last dosing treatment, mice were euthanized with an overdose of sodium pentobarbital solution, and a quantitative amount of wound tissue was collected and homogenized in Triton X-100 (1‰ in PBS). The homogenate was serially diluted and planted on LB agar plates and incubated for 14 hours at 37°C

for colony counting to quantify the number of bacteria in each wound. Next, representative wound tissues were collected for histological analysis following standard staining procedures.

Preparation of MRSA infection contact lens

Contact lens sheets for biofilm culture were cut into circles of 3.5 mm in diameter, placed in 96-well plates with 150 μl of MH medium, and soaked for 12 hours. Then, the contact lenses were transferred to a new 96-well plate, and 150 μl of bacterial suspension (10^5 CFU/ml in MH medium) was added to each well and incubated at 37°C with shaking for 2 hours. After removing the culture suspension and washing the lens with PBS to remove all nonadherent cells, 150 μl of fresh MH medium was added into each well. The plate was incubated at 37°C with shaking for 18 hours to form biofilm on the lenses.

Murine keratitis model

The infection model was conducted by following the previously published method with slight modifications (66, 67). Twelve male BALB/c mice (21 to 24 g) were used in the MRSA-infected keratitis model. Mice were anesthetized by intraperitoneal injection of pentobarbital sodium at a single dose of 75 mg/kg. The eyes of the mice were anesthetized with 0.5% lidocaine hydrochloride drops and subsequently exposed with a lid opener. Two-millimeter-diameter circular filter paper containing 1 μl of 1-heptanol was placed in the center of the eye to disrupt the corneal epithelium. The corneal epithelium was scraped off with an iris restorer, and the eyes were irrigated with 10 ml of saline to remove any debris and remaining 1-heptanol. A contact lens with MRSA biofilm was placed on the damaged corneal surface, and the eyelids were sutured with ophthalmic surgical sutures to ensure that the lens with biofilm cannot slip out of the eye. After 14 hours of infection, these mice with the sutures and contact lens removed were divided into three groups randomly, followed by treatment with 10 μl of different solutions: saline (placebo, negative control), $\beta Lys_{50}HG_{50}$ (400 × MIC), and vancomycin (400 × MIC, positive control) every 5 min during the first hour and every 30 min for the next 7 hours. Thirty minutes after the last dose, the eyeball was collected and homogenized in Triton X-100 (1‰ in PBS), serially diluted, planted on LB agar plates, and incubated for 14 hours at 37°C for colony counting to quantify the number of bacteria on every eyeball. Next, representative eyeballs were collected for histological analysis following standard H&E staining procedures.

Murine neutropenic thigh infection model

The infection model was conducted by following the previously published method with slight modifications (68, 69). Eighteen female ICR mice (22 to 25 g) were used in the neutropenic thigh MRSA infection model. Mice were made neutropenic by two intraperitoneal injection of cyclophosphamide at a concentration of 150 mg/kg on day 4 and 100 mg/kg on day 1 before the infection, respectively.

S. aureus USA300 LAC was cultured in LB medium at 37°C for 10 hours and washed three times with saline after removing the medium. The resulting bacteria were resuspended in 3 ml of saline for later use. Hair was removed from the right thigh of the anesthetized mice, and then the skin was disinfected with iodophor. Mice were infected by intramuscular injection of 30 μl of *S. aureus* USA300 LAC suspension containing $1 × 10^5$ CFU per thigh. After

2 hours of infection, these mice were divided into three groups randomly and treated every 3 hours in 24 hours with different solutions: saline (placebo, the negative control), $\beta Lys_{50}HG_{50}$ (5 mg/ml), and vancomycin (5 mg/ml, the positive control). At 24 hours after the initial treatment, mice were euthanized with an overdose of sodium pentobarbital, and a quantitative amount of muscle tissue was collected and homogenized in Triton X-100 (1‰ in PBS) aseptically. The homogenate was diluted serially, and then 30 μl of each dilution was transferred to LB agar plates, followed by incubation for 14 hours at 37°C to perform colony counting and quantify the load of colonies in per unit mass of thigh tissue. Next, representative thigh tissues were collected for histological analysis following standard staining procedures.

Murine lung infection model

The infection model was conducted by following the previously published method with slight modifications (68, 69). Eighteen female ICR mice (22 to 25 g) were used in the MRSA lung infection model after acclimatizing for 3 days. Mice were made neutropenic by two intraperitoneal injections of cyclophosphamide at a concentration of 150 mg/kg on day 4 and 100 mg/kg on day 1 before the infection, respectively.

S. aureus USA300 LAC was cultured in LB medium at 37°C for 10 hours and washed three times with saline after removing the medium. The obtained bacteria were resuspended in 3 ml of saline for later use. The mice were anesthetized by avertin and infected with 30 μl of *S. aureus* USA300 LAC suspension ($5 × 10^7$ CFU/ml) by intratracheal instillation. After 2 hours of infection, these mice were divided into three groups randomly and treated intratracheally for two times with 12-hour intervals using a small nebulizer needle (Liquid Aerosol Devices, MicroSprayer Aerosolizers, Shanghai TOW Intelligent Technology Co. Ltd.) with saline (placebo, the negative control), $\beta Lys_{50}HG_{50}$ (4 mg/ml), and vancomycin (4 mg/ml, the positive control). Mice were euthanized with an overdose of sodium pentobarbital solution, and then the lung tissue was collected and homogenized in Triton X-100 (1‰ in PBS). The homogenate was serially diluted on the LB agar and incubated at 37°C for 14 hours. The number of colonies on the plate was counted, from which the load of colonies in per unit mass of lung tissue can be calculated. Next, representative lung tissues were collected for histological analysis following standard staining procedures.

Murine peritonitis model

The infection model was conducted by following the previously published method with slight modifications (58, 70). *S. aureus* USA300 LAC was cultured in LB medium at 37°C for 10 hours and washed three times with saline after removing the medium and resuspended in saline for use. Twenty-four female ICR mice (21 to 24 g) were used in the MRSA peritonitis model. Mice were infected by intraperitoneal injection with 0.2 ml of *S. aureus* USA300 LAC suspension ($1.5 × 10^9$ CFU/ml) that was resuspended in saline containing 5% mucin. Half an hour after preinfection, six of the mice were euthanized by intraperitoneal injection of an overdose of sodium pentobarbital. Peritoneal lavage was performed by injecting 3 ml of saline into the abdominal cavity and massaging the abdomen. The abdominal cavity was opened with a scalpel, and the lavage fluid was removed from the abdomen for colony counting. Blood was collected by cardiac puncture and analyzed for colony

counting. Then, vital organs, including heart, liver, spleen, lung, and kidney, were collected and homogenized in Triton X-100 (1‰ in PBS). The homogenate was serially diluted on the LB agar and incubated at 37°C for 14 hours. The number of colonies on the plate was counted, from which the load of colonies in per unit mass of organ or per unit volume of blood and lavage fluid can be calculated.

The remaining 18 preinfected mice were divided into three groups randomly and treated by intraperitoneal injections of saline (placebo, negative control), $\beta Lys_{50}HG_{50}$ (40 mg/kg), and vancomycin (40 mg/kg) and monitored for the next 48 hours. As soon as the infected mice died, their vital organs, blood, and lavage fluid were collected, and colony counting was performed according to the previous procedure. Surviving mice were euthanized at 48 hours after infection, and colony counting was performed according to the same procedure. In addition, the same organs from different treatment groups were collected and fixed for histological analysis of H&E staining. The survival experiment of infected mice after treatment was conducted independently, and infected mice were observed for 7 days after treatment for their physiological status, while survival was recorded.

Polypeptide toxicity evaluation in vivo
The in vivo toxicity evaluation model was conducted by following the previously published method with slight modifications (71). Eighteen female ICR mice (23 to 25 g) were used in the toxicity evaluation of $\beta Lys_{50}HG_{50}$ and poly-β-lysine. These mice were divided into three groups randomly, and $\beta Lys_{50}HG_{50}$ (40 mg/kg), poly-β-lysine (12.5 mg/kg), and saline were injected via tail vein. After normal feeding for 2 and 14 days, blood (1 ml) was collected from mice by cardiac puncture, during which body weight was recorded. Serum biochemical indices including ALT, AST, CREA, urea nitrogen, and sodium and potassium ion levels in blood were analyzed. Mice were euthanized with an overdose of sodium pentobarbital solution, and the liver and kidney were collected for histological analysis following standard staining procedures.

Supplementary Materials
This PDF file includes:
Supplementary Text
Figs. S1 to S40

View/request a protocol for this paper from *Bio-protocol*.

REFERENCES AND NOTES
1. L. El Haddad, C. P. Harb, M. A. Gebara, M. A. Stibich, R. F. Chemaly, A systematic and critical review of bacteriophage therapy against multidrug-resistant ESKAPE organisms in humans. *Clin. Infect. Dis.* **69**, 167–178 (2019).
2. A. Harms, E. Maisonneuve, K. Gerdes, Mechanisms of bacterial persistence during stress and antibiotic exposure. *Science* **354**, aaf4268 (2016).
3. R. L. Mork, P. G. Hogan, C. E. Muenks, M. G. Boyle, R. M. Thompson, M. L. Sullivan, J. J. Morelli, J. Seigel, R. C. Orscheln, J. Bubeck Wardenburg, S. J. Gehlert, C.-A. D. Burnham, A. Rzhetsky, S. A. Fritz, Longitudinal, strain-specific *Staphylococcus aureus* introduction and transmission events in households of children with community-associated meticillin-resistant *S aureus* skin and soft tissue infection: A prospective cohort study. *Lancet Infect. Dis.* **20**, 188–198 (2020).
4. N. A. Turner, B. K. Sharma-Kuinkel, S. A. Maskarinec, E. M. Eichenberger, P. P. Shah, M. Carugati, T. L. Holland, V. G. Fowler, Methicillin-resistant *Staphylococcus aureus*: An overview of basic and clinical research. *Nat. Rev. Microbiol.* **17**, 203–218 (2019).
5. H. Boucher, L. G. Miller, R. R. Razonable, Serious infections caused by methicillin-resistant *Staphylococcus aureus*. *Clin. Infect. Dis.* **51**, S183–S197 (2010).
6. R. S. Daum, Skin and soft-tissue infections caused by *Methicillin-Resistant Staphylococcus aureus*. *N. Engl. J. Med.* **357**, 380–390 (2007).
7. C. R. Arciola, D. Campoccia, L. Montanaro, Implant infections: Adhesion, biofilm formation and immune evasion. *Nat. Rev. Microbiol.* **16**, 397–409 (2018).
8. K. Lewis, The science of antibiotic discovery. *Cell* **181**, 29–45 (2020).
9. R. Nelson, Antibiotic development pipeline runs dry. *Lancet* **362**, 1726–1727 (2003).
10. R. E. Hancock, H.-G. Sahl, Antimicrobial and host-defense peptides as new anti-infective therapeutic strategies. *Nat. Biotechnol.* **24**, 1551–1557 (2006).
11. M. Magana, M. Pushpanathan, A. L. Santos, L. Leanse, M. Fernandez, A. Ioannidis, M. A. Giulianotti, Y. Apidianakis, S. Bradfute, A. L. Ferguson, A. Cherkasov, M. N. Seleem, C. Pinilla, C. de la Fuente-Nunez, T. Lazaridis, T. Dai, R. A. Houghten, R. E. W. Hancock, G. P. Tegos, The value of antimicrobial peptides in the age of resistance. *Lancet Infect. Dis.* **20**, e216–e230 (2020).
12. N. Mookherjee, M. A. Anderson, H. P. Haagsman, D. J. Davidson, Antimicrobial host defence peptides: Functions and clinical potential. *Nat. Rev. Drug Discov.* **19**, 311–332 (2020).
13. B. L. Bray, Large-scale manufacture of peptide therapeutics by chemical synthesis. *Nat. Rev. Drug Discov.* **2**, 587–593 (2003).
14. M. Sieprawska-Lupa, P. Mydel, K. Krawczyk, K. Wojcik, M. Puklo, B. Lupa, P. Suder, J. Silberring, M. Reed, J. Pohl, W. Shafer, F. McAleese, T. Foster, J. Travis, J. Potempa, Degradation of human antimicrobial peptide LL-37 by *Staphylococcus aureus*-derived proteinases. *Antimicrob. Agents Chemother.* **48**, 4673–4679 (2004).
15. E. A. Porter, X. Wang, H. S. Lee, B. Weisblum, S. H. Gellman, Erratum: Non-haemolytic β-amino-acid oligomers. *Nature* **405**, 298 (2000).
16. M. Zasloff, Antimicrobial peptides of multicellular organisms. *Nature* **415**, 389–395 (2002).
17. X. Li, H. T. Bai, Y. C. Yang, J. Yoon, S. Wang, X. Zhang, Supramolecular antibacterial materials for combatting antibiotic resistance. *Adv. Mater.* **31**, 1805092 (2019).
18. Y. Wu, G. Xia, W. Zhang, K. Chen, Y. Bi, S. Liu, W. Zhang, R. Liu, Structural design and antimicrobial properties of polypeptides and saccharide–polypeptide conjugates. *J. Mater. Chem. B* **8**, 9173–9196 (2020).
19. D. H. Liu, W. F. DeGrado, De novo design, synthesis, and characterization of antimicrobial β-peptides. *J. Am. Chem. Soc.* **123**, 7553–7559 (2001).
20. B. P. Mowery, S. E. Lee, D. A. Kissounko, R. F. Epand, R. M. Epand, B. Weisblum, S. S. Stahl, S. H. Gellman, Mimicry of antimicrobial host-defense peptides by random copolymers. *J. Am. Chem. Soc.* **129**, 15474–15476 (2007).
21. C. Ghosh, P. Sarkar, S. Samaddar, D. Uppu, J. Haldar, L-Lysine based lipidated biphenyls as agents with anti-biofilm and anti-inflammatory properties that also inhibit intracellular bacteria. *Chem. Commun.* **53**, 8427–8430 (2017).
22. C. Krumm, S. Harmuth, M. Hijazi, B. Neugebauer, A.-L. Kampmann, H. Geltenpoth, A. Sickmann, J. C. Tiller, Antimicrobial poly(2-methyloxazoline)s with bioswitchable activity through satellite group modification. *Angew. Chem. Int. Ed. Engl.* **53**, 3830–3834 (2014).
23. Z. Y. Si, H. W. Lim, M. Y. F. Tay, Y. Du, L. Ruan, H. F. Qiu, R. Zamudio-Vazquez, S. Reghu, Y. H. Chen, W. S. Tiong, K. Marimuthu, P. P. De, O. T. Ng, Y. B. Zhu, Y.-H. Gan, Y. R. Chi, H. W. Duan, G. C. Bazan, E. P. Greenberg, M. B. Chan-Park, K. Pethe, A glycosylated cationic block poly(β-peptide) reverses intrinsic antibiotic resistance in all ESKAPE gram-negative bacteria. *Angew. Chem. Int. Ed.* **59**, 6819–6826 (2020).
24. Y. Shi, P. Teng, P. Sang, F. She, L. Wei, J. Cai, γ-AApeptides: Design, structure, and applications. *Acc. Chem. Res.* **49**, 428–441 (2016).
25. B. Mishra, S. Reiling, D. Zarena, G. Wang, Host defense antimicrobial peptides as antibiotics: Design and application strategies. *Curr. Opin. Chem. Biol.* **38**, 87–96 (2017).
26. W. Chin, G. Zhong, Q. Pu, C. Yang, W. Lou, P. F. De Sessions, B. Periaswamy, A. Lee, Z. C. Liang, X. Ding, S. Gao, C. W. Chu, S. Bianco, C. Bao, Y. W. Tong, W. Fan, M. Wu, J. L. Hedrick, Y. Y. Yang, A macromolecular approach to eradicate multidrug resistant bacterial infections while mitigating drug resistance onset. *Nat. Commun.* **9**, 917 (2018).
27. S. Chen, X. Shao, X. Xiao, Y. Dai, Y. Wang, J. Xie, W. Jiang, Y. Sun, Z. Cong, Z. Qiao, H. Zhang, L. Liu, Q. Zhang, W. Zhang, L. Zheng, B. Yu, M. Chen, W. Cui, J. Fei, R. Liu, Host defense peptide mimicking peptide polymer exerting fast, broad spectrum, and potent activities toward clinically Isolated multidrug-resistant bacteria. *ACS Infect. Dis.* **6**, 479–488 (2020).
28. Q. Zhang, P. Ma, J. Xie, S. Zhang, X. Xiao, Z. Qiao, N. Shao, M. Zhou, W. Zhang, C. Dai, Y. Qian, F. Qi, R. Liu, Host defense peptide mimicking poly-β-peptides with fast, potent and broad spectrum antibacterial activities. *Biomater. Sci.* **7**, 2144–2151 (2019).
29. Y. Wu, D. Zhang, P. Ma, R. Zhou, L. Hua, R. Liu, Lithium hexamethyldisilazide initiated superfast ring opening polymerization of alpha-amino acid N-carboxyanhydrides. *Nat. Commun.* **9**, 5297 (2018).
30. J. Sun, M. Li, M. Lin, B. Zhang, X. Chen, High antibacterial activity and selectivity of the versatile polysulfoniums that combat drug resistance. *Adv. Mater.* **33**, 2104402 (2021).

31. B. P. Mowery, A. H. Lindner, B. Weisblum, S. S. Stahl, S. H. Gellman, Structure–activity relationships among random nylon-3 copolymers that mimic antibacterial host-defense peptides. *J. Am. Chem. Soc.* **131**, 9735–9745 (2009).

32. R. Liu, X. Chen, S. P. Falk, B. P. Mowery, A. J. Karlsson, B. Weisblum, S. P. Palecek, K. S. Masters, S. H. Gellman, Structure–activity relationships among antifungal nylon-3 polymers: Identification of materials active against drug-resistant strains of *Candida albicans*. *J. Am. Chem. Soc.* **136**, 4333–4342 (2014).

33. R. Liu, X. Chen, S. Chakraborty, J. J. Lemke, Z. Hayouka, C. Chow, R. A. Welch, B. Weisblum, K. S. Masters, S. H. Gellman, Tuning the biological activity profile of antibacterial polymers via subunit substitution pattern. *J. Am. Chem. Soc.* **136**, 4410–4418 (2014).

34. K. Zhang, Y. Du, Z. Si, Y. Liu, M. E. Turvey, C. Raju, D. Keogh, L. Ruan, S. L. Jothy, S. Reghu, K. Marimuthu, P. P. De, O. T. Ng, J. R. Mediavilla, B. N. Kreiswirth, Y. R. Chi, J. Ren, K. C. Tam, X.-W. Liu, H. Duan, Y. Zhu, Y. Mu, P. T. Hammond, G. C. Bazan, K. Pethe, M. B. Chan-Park, Enantiomeric glycosylated cationic block co-beta-peptides eradicate *Staphylococcus aureus* biofilms and antibiotic-tolerant persisters. *Nat. Commun.* **10**, 4792 (2019).

35. M. Venkatesh, V. A. Barathi, E. T. L. Goh, R. Anggara, M. Fazil, A. J. Y. Ng, S. Harini, T. T. Aung, S. J. Fox, S. Liu, L. Yang, T. M. S. Barkham, X. J. Loh, N. K. Verma, R. W. Beuerman, R. Lakshminarayanan, Antimicrobial activity and cell selectivity of synthetic and biosynthetic cationic polymers. *Antimicrob. Agents Chemother.* **61**, e00469-17 (2017).

36. D. Pranantyo, L. Q. Xu, Z. Hou, E.-T. Kang, M. B. Chan-Park, Increasing bacterial affinity and cytocompatibility with four-arm star glycopolymers and antimicrobial α-polylysine. *Polym. Chem.* **8**, 3364–3373 (2017).

37. M. Xiong, M. W. Lee, R. A. Mansbach, Z. Song, Y. Bao, R. M. Peek Jr., C. Yao, L.-F. Chen, A. L. Ferguson, G. C. Wong, J. Cheng, Helical antimicrobial polypeptides with radial amphiphilicity. *Proc. Natl. Acad. Sci. U.S.A.* **112**, 13155–13160 (2015).

38. M. Xiong, Z. Han, Z. Song, J. Yu, H. Ying, L. Yin, J. Cheng, Bacteria-assisted activation of antimicrobial polypeptides by a random-coil to helix transition. *Angew. Chem. Int. Ed.* **56**, 10826–10829 (2017).

39. C. D. Fjell, J. A. Hiss, R. E. Hancock, G. Schneider, Designing antimicrobial peptides: Form follows function. *Nat. Rev. Drug Discov.* **11**, 37–51 (2011).

40. M. Zhou, Y. Qian, J. Xie, W. Zhang, W. Jiang, X. Xiao, S. Chen, C. Dai, Z. Cong, Z. Ji, N. Shao, L. Liu, Y. Wu, R. Liu, Poly(2-Oxazoline)-based functional peptide mimics: Eradicating MRSA infections and persisters while alleviating antimicrobial resistance. *Angew. Chem. Int. Ed.* **59**, 6412–6419 (2020).

41. C. Dai, M. Zhou, W. Jiang, X. Xiao, J. Zou, Y. Qian, Z. Cong, Z. Ji, L. Liu, J. Xie, Z. Qiao, R. Liu, Breaking or following the membrane-targeting mechanism: Exploring the antibacterial mechanism of host defense peptide mimicking poly(2-oxazoline)s. *J. Mater. Sci. Technol.* **59**, 220–226 (2020).

42. M. Zhou, W. Jiang, J. Xie, W. Zhang, Z. Ji, J. Zou, Z. Cong, X. Xiao, J. Gu, R. Liu, Peptide-mimicking poly(2-oxazoline)s displaying potent antimicrobial properties. *ChemMedChem* **16**, 309–315 (2021).

43. S. Chakraborty, R. Liu, Z. Hayouka, X. Chen, J. Ehrhardt, Q. Lu, E. Burke, Y. Yang, B. Weisblum, G. C. Wong, K. S. Masters, S. H. Gellman, Ternary nylon-3 copolymers as host-defense peptide mimics: Beyond hydrophobic and cationic subunits. *J. Am. Chem. Soc.* **136**, 14530–14535 (2014).

44. H. Huang, N. Iwasawa, T. Mukaiyama, A convenient method for the construction of β-lactam compounds from β-amino acids using 2-chloro-1-methylpyridinium iodide as condensing reagent. *Chem. Lett.* **13**, 1465–1466 (1984).

45. R. A. Fisher, S. Gollan, S. Helaine, Persistent bacterial infections and persister cells. *Nat. Rev. Microbiol.* **15**, 453–464 (2017).

46. A. G. Dale, J. Hinds, J. Mann, P. W. Taylor, S. Neidle, Symmetric bis-benzimidazoles are potent anti-staphylococcal agents with dual inhibitory mechanisms against DNA gyrase. *Biochemistry* **51**, 5860–5871 (2012).

47. R. K. Flamm, D. J. Farrell, P. R. Rhomberg, N. E. Scangarella-Oman, H. S. Sader, Gepotidacin (GSK2140944) in vitro activity against Gram-positive and Gram-negative bacteria. *Antimicrob. Agents Chemother.* **61**, e00468-17 (2017).

48. W. H. Hu, R. W. Burli, J. A. Kaizerman, K. W. Johnson, M. I. Gross, M. Iwamoto, P. Jones, D. Lofland, S. Difuntorum, H. Chen, B. Bozdogan, P. C. Appelbaum, H. E. Moser, DNA binding ligands with improved in vitro and in vivo potency against drug-resistant *Staphylococcus aureus*. *J. Med. Chem.* **47**, 4352–4355 (2004).

49. D. J. Dwyer, P. A. Belenky, J. H. Yang, I. C. MacDonald, J. D. Martell, N. Takahashi, C. T. Chan, M. A. Lobritz, D. Braff, E. G. Schwarz, J. D. Ye, M. Pati, M. Vercruysse, P. S. Ralifo, K. R. Allison, A. S. Khalil, A. Y. Ting, G. C. Walker, J. J. Collins, Antibiotics induce redox-related physiological alterations as part of their lethality. *Proc. Natl. Acad. Sci. U.S.A.* **111**, E2100–E2109 (2014).

50. Y. Hong, J. Zeng, X. Wang, K. Drlica, X. Zhao, Post-stress bacterial cell death mediated by reactive oxygen species. *Proc. Natl. Acad. Sci. U.S.A.* **116**, 10064–10071 (2019).

51. M. A. Kang, E.-Y. So, A. L. Simons, D. R. Spitz, T. Ouchi, DNA damage induces reactive oxygen species generation through the H2AX-Nox1/Rac1 pathway. *Cell Death Dis.* **3**, e249 (2012).

52. P. T. Dong, H. Mohammad, J. Hui, L. G. Leanse, J. Li, L. Liang, T. Dai, M. N. Seleem, J.-X. Cheng, Photolysis of staphyloxanthin in methicillin-resistant *Staphylococcus aureus* potentiates killing by reactive oxygen species. *Adv. Sci.* **6**, 1900030 (2019).

53. X. Zhang, Z. Zhang, Q. Shu, C. Xu, Q. Zheng, Z. Guo, C. Wang, Z. Hao, X. Liu, G. Wang, W. Yan, H. Chen, C. Lu, Copper clusters: An effective antibacterial for eradicating multidrug-resistant bacterial infection in vitro and in vivo. *Adv. Funct. Mater.* **31**, 2008720 (2021).

54. M. Lu, S. Wang, T. Wang, S. Hu, B. Bhayana, M. Ishii, Y. Kong, Y. Cai, T. Dai, W. Cui, M. X. Wu, Bacteria-specific phototoxic reactions triggered by blue light and phytochemical carvacrol. *Sci. Transl. Med.* **13**, eaba3571 (2021).

55. L. Brown, J. M. Wolf, R. Prados-Rosales, A. Casadevall, Through the wall: Extracellular vesicles in Gram-positive bacteria, mycobacteria and fungi. *Nat. Rev. Microbiol.* **13**, 620–630 (2015).

56. M. Toyofuku, N. Nomura, L. Eberl, Types and origins of bacterial membrane vesicles. *Nat. Rev. Microbiol.* **17**, 13–24 (2019).

57. R. Bouley, M. Kumarasiri, Z. Peng, L. H. Otero, W. Song, M. A. Suckow, V. A. Schroeder, W. R. Wolter, E. Lastochkin, N. T. Antunes, H. Pi, S. Vakulenko, J. A. Hermoso, M. Chang, S. Mobashery, Discovery of antibiotic (E)-3-(3-Carboxyphenyl)-2-(4-cyanostyryl)quinazolin-4(3H)-one. *J. Am. Chem. Soc.* **137**, 1738–1741 (2015).

58. S. J. Lam, N. M. O'Brien-Simpson, N. Pantarat, A. Sulistio, E. H. H. Wong, Y.-Y. Chen, J. C. Lenzo, J. A. Holden, A. Blencowe, E. C. Reynolds, G. G. Qiao, Combating multidrug-resistant Gram-negative bacteria with structurally nanoengineered antimicrobial peptide polymers. *Nat. Microbiol.* **1**, 16162 (2016).

59. D. Nagarajan, N. Roy, O. Kulkarni, N. Nanajkar, A. Datey, S. Ravichandran, C. Thakur, T. Sandeep, I. V. Aprameya, S. P. Sarma, D. Chakravortty, N. Chandra, Ω76: A designed antimicrobial peptide to combat carbapenem- and tigecycline-resistant *Acinetobacter baumannii*. *Sci. Adv.* **5**, eaax1946 (2019).

60. A. L. Esposito, R. A. Gleckman, Vancomycin. A second look. *JAMA* **238**, 1756–1757 (1977).

61. E. J. Filippone, W. K. Kraft, J. L. Farber, The nephrotoxicity of vancomycin. *Clin. Pharmacol. Ther.* **102**, 459–469 (2017).

62. M. Benincasa, Q. Barrière, G. Runti, O. Pierre, M. Bourge, M. Scocchi, P. Mergaert, Single cell flow cytometry assay for peptide uptake by bacteria. *Bio-Protocol* **6**, e2038 (2016).

63. Z. Jiang, Y. Liu, R. Shi, X. Feng, W. Xu, X. Zhuang, J. Ding, X. Chen, Versatile polymer-initiating biomineralization for tumor blockade therapy. *Adv. Mater.* **34**, 2110094 (2022).

64. A. Antonoplis, X. Zang, M. A. Huttner, K. K. L. Chong, Y. B. Lee, J. Y. Co, M. R. Amieva, K. A. Kline, P. A. Wender, L. Cegelski, A dual-function antibiotic-transporter conjugate exhibits superior activity in sterilizing MRSA biofilms and killing persister cells. *J. Am. Chem. Soc.* **140**, 16140–16151 (2018).

65. L. Zheng, J. Li, M. Yu, W. Jia, S. Duan, D. Cao, X. Ding, B. Yu, X. Zhang, F.-J. Xu, Molecular sizes and antibacterial performance relationships of flexible ionic liquid derivatives. *J. Am. Chem. Soc.* **142**, 20257–20269 (2020).

66. S. Obuobi, V. Mayandi, N. A. M. Nor, B. J. Lee, R. Lakshminarayanan, P. L. R. Ee, Nucleic acid peptide nanogels for the treatment of bacterial keratitis. *Nanoscale* **12**, 17411–17425 (2020).

67. H.-Y. Lin, S.-W. Wang, J.-Y. Mao, H.-T. Chang, S. G. Harroun, H.-J. Lin, C.-C. Huang, J.-Y. Lai, Carbonized nanogels for simultaneous antibacterial and antioxidant treatment of bacterial keratitis. *Chem. Eng. J.* **411**, 128469 (2021).

68. L. L. Ling, T. Schneider, A. J. Peoples, A. L. Spoering, I. Engels, B. P. Conlon, A. Mueller, T. F. Schaberle, D. E. Hughes, S. Epstein, M. Jones, L. Lazarides, V. A. Steadman, D. R. Cohen, C. R. Felix, K. A. Fetterman, W. P. Millett, A. G. Nitti, A. M. Zullo, C. Chen, K. Lewis, A new antibiotic kills pathogens without detectable resistance. *Nature* **517**, 455–459 (2015).

69. T. F. Durand-Reville, A. A. Miller, J. P. O'Donnell, X. Wu, M. A. Sylvester, S. Guler, R. Iyer, A. B. Shapiro, N. M. Carter, C. Velez-Vega, S. H. Moussa, S. M. McLeod, A. Chen, A. M. Tanudra, J. Zhang, J. Comita-Prevoir, J. A. Romero, H. Huynh, A. D. Ferguson, P. S. Horanyi, S. J. Mayclin, H. S. Heine, G. L. Drusano, J. E. Cummings, R. A. Slayden, R. A. Tommasi, Rational design of a new antibiotic class for drug-resistant infections. *Nature* **597**, 698–702 (2021).

70. M. Song, Y. Liu, X. Huang, S. Ding, Y. Wang, J. Shen, K. Zhu, A broad-spectrum antibiotic adjuvant reverses multidrug-resistant Gram-negative pathogens. *Nat. Microbiol.* **5**, 1040–1050 (2020).

71. J. Lakshmaiah Narayana, B. Mishra, T. Lushnikova, Q. Wu, Y. S. Chhonker, Y. Zhang, D. Zarena, E. S. Salnikov, X. Dang, F. Wang, C. Murphy, K. W. Foster, S. Gorantla, B. Bechinger, D. J. Murry, G. Wang, Two distinct amphipathic peptide antibiotics with systemic efficacy. *Proc. Natl. Acad. Sci. U.S.A.* **117**, 19446–19454 (2020).